Final report submitted to

ONR BAA ONRBAA15-001

Long Range BAA for Navy and Marine Corps Science and Technology Program:

Expeditionary Maneuver Warfare & Combating Terrorism Department (Code 30)

1. Title of Grant: "Remote compact robotic-optical sensor for long range chemical detection"
(ONR Grant # 11848345, Award# N00014-15-1-2575)

2. Prime Offeror: University of Hawaii

3. Principal Investigator: Dr. Anupam K. Misra
Co-Investigators: Dr. Shiv K. Sharma, Dr. John Porter
Collaborator: Mr. Brian Chee

4. Technical contact: Dr. Anupam K. Misra
University of Hawaii
Hawaii Institute of Geophysics & Planetology
1680 East-West Rd, POST #602
Honolulu, HI-96822
Phone: 808-277-5058
Fax: 808-956-3188
E-mail: anupam@hawaii.edu

5. Administrative contact: Kyle Koza
Contracts & Grants Specialist
University of Hawai'i
Office of Research Services
Mānoa Service Center

Phone: 808-956-4054
Fax: 808-956-9081
Email: kkoza@hawaii.edu

6. Period of Performance: 7/1/2015 to 9/30/2018

7. Report submitted by: Anupam Misra
8. Date: Dec 30, 2018

Final report

Contents

1. Background/scope of effort:

Raman spectroscopy is a non-destructive technique for detecting a wide range of materials in any state (solid, liquid, or gas). A Raman spectrum resulting from the vibrational modes of a molecule consists of sharp, well defined narrow spectral lines that are used as fingerprints for identification of chemicals (Ferraro et al., 2003). This technique produces results with a high confidence level and very low incidence of false alarms. The spectral features are unique even for various polymorphs of the same chemical. Raman spectra can detect a wide range of chemicals that are of interest to the ONR, such as explosives (TNT, RDX, C4, TATB, HMX, PETN, various nitrates, chlorates, perchlorates, peroxides, etc.), hazardous materials (benzene, naphthalene, acetone, various acids, gasoline and other flammable materials, etc.), toxic gases and various chemical vapors (Sharma et al., 2005, 2006 a, 2006 b; Misra et al., 2005, 2006 Carter et al., 2005; Gaft and Nagli, 2008; Oxley et al., 2008; Stokes et al., 2008; Wright et al., 2003; Ali et al., 2009, Hokr et al., 2014). A portable stand-off Raman system is one of the techniques demonstrated to detect the molecular fingerprints of inorganic, organic and explosive materials at 10 to 120 meter distances from the Raman spectrograph (Sharma et al., 2003 a; 2003 b; 2004; 2014, Misra et al., 2005, 2006; 2007, 2010, 2012a, b, Porter et al., 2012).

With previous funding from the ONR, the University of Hawaii developed a state of the art remote Raman+LIBS system. The remote Raman+LIBS system, which uses an 8 inch telescope, has been successfully field tested for detection of various chemicals using Raman spectroscopy from 120 m distance using only one laser shot excitation and 100 ns detection time (Misra et al., 2012). The same system was recently used by Acosta-Maeda et al. (2016) to detect various chemicals using a Raman signal from a distance of 430 m distance during a bright afternoon with the sun shining on the samples and integration time of 1 to 10 s. The range for performing standoff LIBS measurements from this system is currently 50 m when using full laser energy of 100 mJ/pulse at 532 nm. The upper range of standoff LIBS is limited because of the challenges in focusing the laser above the required laser power density to obtain molecular breakdown at longer distances. Using very high-powered lasers and large telescopes, standoff LIBS has been demonstrated at distance of 130 meters (Fortes et al., 2010).

In general, the overall sizes of the remote Raman and LIBS systems increase to achieve longer detection range for direct interrogation of the targets. From a safety and field operation point of view, it is highly desirable to develop remote chemical detection systems that are small, use low laser power, and also have detection ranges of several hundred meters to perform chemical detection from a safe distance.

Under this ONR project we developed a novel approach for performing long range chemical detection using low laser pulse power and short integration time. The method is based on two parts system, namely an Active Transmitter-Receiver (ATR) sensor (part a) combined with a mobile distant Focusing Rover (FR) (part b). The ATR is a compact remote Raman system which uses low laser pulse energy of 3 mJ/pulse for sample excitation and a 3” collection optics for recording remote Raman spectra. The system is also able to perform standoff LIBS. The ATR directs a collimated or slightly diverging laser beam towards the distant FR where the laser beam is redirected and focused onto a nearby target. The scattered light generated by the target is collected by the FR and sent back to the ATR as a slightly diverging beam for spectral analysis and chemical identification. Using this method, significant improvement in remote Raman and LIBS signals is achieved.

2. Executive Summary

In the field of remote chemical detection using active laser interrogation, it is generally accepted that for a longer detection range, the size of the system must be larger in order to compensate for the signal loss due to the lower cross-section of collection optics. Using 8" diameter telescope and 100 mJ/pulse laser power, we have successfully detected various chemicals from a distance of 430 m using Raman spectroscopy. To the best of our knowledge, Dr. Laserna's group in Spain (Univ. of Malaga) holds the world record for conducting LIBS at the distance of 130 m using a large system utilizing a pulsed laser with 750 mJ/pulse at 1064 nm.

Under this research project, we developed a novel two component approach that helps to obtain remote Raman and LIBS spectra of targets at distance of 246 m with 3 mJ/pulse in daytime and fast detection time of 1 s using a small remote Raman+LIBS system with 3" diameter collection optics. The two components of the method are: (i) a small spectroscopy system utilizing 76 mm diameter collection optics and (ii) a small remote lens near the target. Remote Raman spectra of various chemicals could be obtained with integration time of 1 s. Remote LIBS spectra of minerals from a distance of 246 m were obtained using single laser pulse of 3 mJ/pulse energy. This is a new world record for performing remote LIBS and also using low laser pulse energy. This method is also applicable for developing future eye safe remote LIBS system using low power lasers in the IR region, e.g. 1550 nm laser.

This research work demonstrates a simple approach that significantly improves remote Raman and LIBS capabilities for long range chemical detection with compact low laser power Raman and LIBS systems.

3. Technical Contents and data

3.1 Working principle (methodology):

Figure 1 illustrates a two-component approach to performing remote Raman and LIBS measurements of a distant target. The two components of the system are (1) a compact remote Raman and LIBS system and (2) a focusing lens.

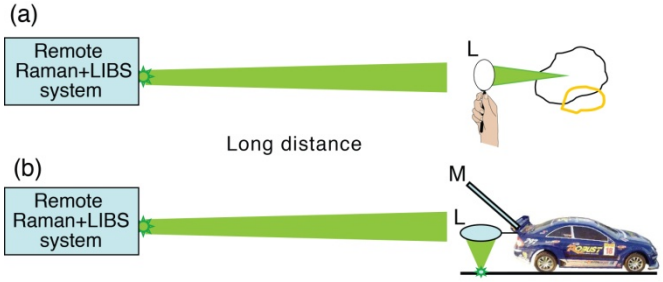

Figure 1. Schematic diagram showing two-component system for remote chemical analysis using a compact remote Raman+LIBS system and distant focusing lens (L) near the target. Geometry (a) for analyzing vertical surfaces and geometry (b) for analyzing chemicals on ground using a folding mirror (M).

The remote Raman+LIBS system sends out a collimated (or slightly diverging) laser beam towards the distant focusing lens. The lens focuses the laser on the target of interest and sends back Raman and LIBS signals towards the system. For chemical targets lying on the ground, a

folding mirror can be used in combination with the lens as shown in Fig. 1(b). The lens can be carried to the distant target by a person, remote controlled car, or unmanned aerial vehicle (UAV). For geological surveys and field operations, the field worker only needs to carry a lens and a mirror to various target sites. This allows quick chemical analysis of various samples in the field without collecting samples and without moving the main remote Raman+LIBS system, which can stay inside a vehicle or rover.

3.2 System development:

Under this project, we developed two compact remote Raman systems as shown in Figure 2 and 3. Figure 2 shows a compact remote Raman system with 1" diameter collection lens.

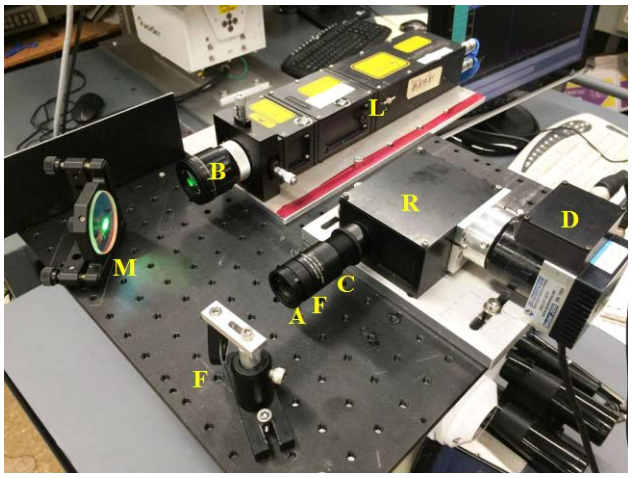

Figure 2. Compact remote Raman system with 1" collection optics. The various components of the systems are: L-532 nm pulsed laser; B-3x laser beam expander; M-laser mirror; F-long pass Raman filter; A-iris aperture; C-1" collection lens; R-compact Raman spectrograph; and D-mini ICCD detector. Breadboard screw holes are 1" apart.

Figure 3 shows another version of a compact remote Raman system utilizing a small 3" mirror lens as collection optics, instead of 1" lens, for better collection of backscattered Raman signal.

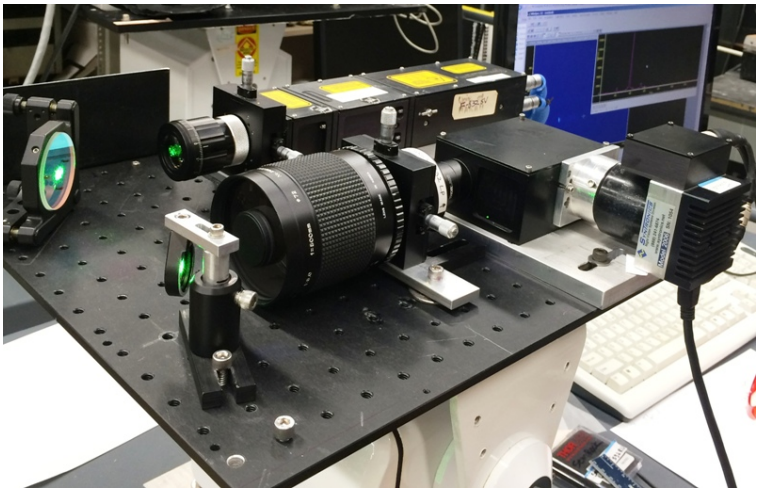

Figure 3. Compact remote Raman system with a small 3" mirror lens as collection optics.

The small 3" diameter mirror lens is available at low cost and does not significantly increase the overall system size. Both systems were tested in the lab for performance.

3.3 Laboratory testing:

Figure 4 shows the lab setting for remote Raman detection from a distance of 20 m with all room lights turned on. The system performances were tested with and without the help of a focusing lens (a small lens to be placed on a rover).

Figure 4. Lab setting for testing remote Raman system at 20 m target distance under bright condition. Targets are located on the far side of the room where green laser spot is visible.

Figure 5 shows the detection capability of the system (shown in Fig. 2) to detect ammonium nitrate from a distance of 20 m using only 3 mJ/pulse of laser power and 1 s integration time with direct interrogation. The iris aperture of the system for this experiment was closed to 0.5" diameter opening. The ICCD image shows weak detection of the target ammonium nitrate along with detection of atmospheric gases (oxygen and nitrogen). The compact remote Raman system recorded the entire Raman signal from 150 cm^{-1} to 4500 cm^{-1}. The resolution of the system was increased by recording the Raman signal in two spectral images on the same detector. The bottom spectral image covers the spectral range of 150 cm^{-1} to 2500 cm^{-1} and the top image covers the higher frequency region from 2400- 4500 cm^{-1}. The image was processed to produce Raman spectra using custom software previously developed under the ONR program. Figure 6 shows the Raman spectrum of the target along with atmospheric gases from the image data shown in Fig. 5.

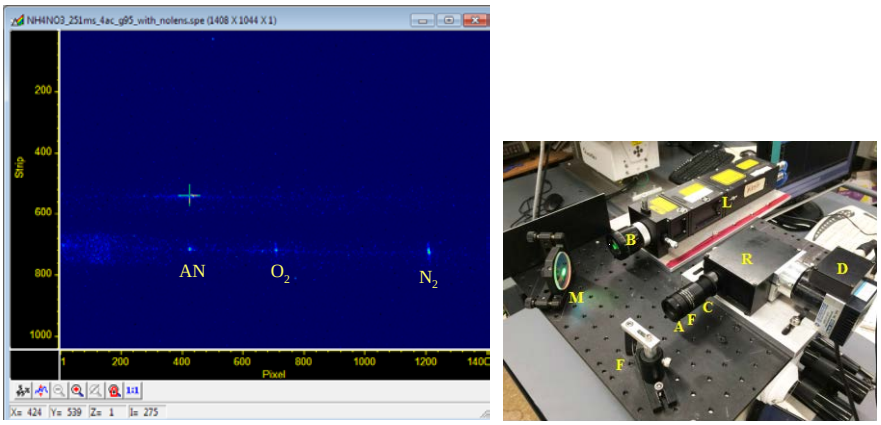

Figure 5. Direct detection of ammonium nitrate from 20 m distance using 0.5 inch diameter collection optics (system setup shown on right frame). Laser power 3 mJ/pulse, 20Hz, 1 second integration time.

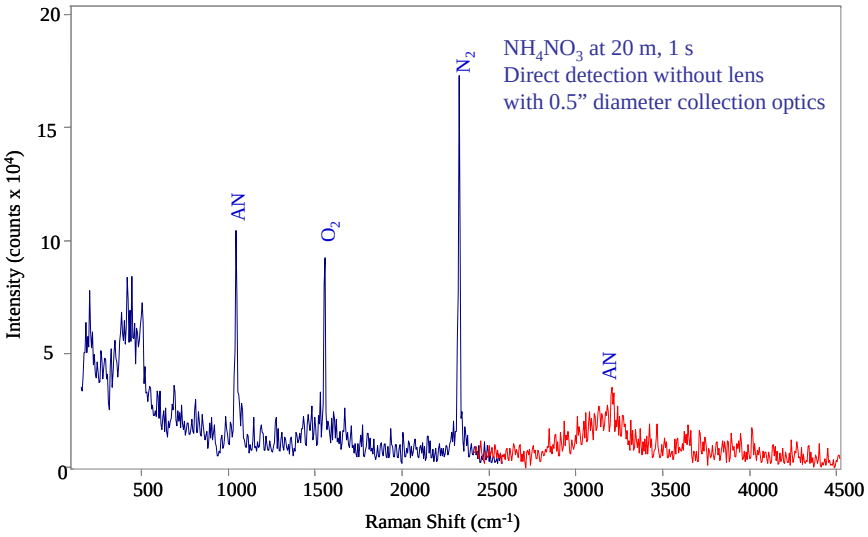

Figure 6. Raman spectrum generated from ICCD image shown in Fig. 5. Direct detection of ammonium nitrate from 20 m distance using 0.5 inch diameter collection optics. Laser power 3 mJ/pulse, 20 Hz, 1 second integration time.

It was determined from the lab testing that the remote Raman system using 3" diameter telescope as collection optics (shown in Fig. 3) has significantly better performance in comparison to the system with 1" collection lens (Fig. 2). Figure 7 shows the single pulse detection of KNO_3 sample from 20 m distance using a 3" mirror lens as collection optics (system shown in Fig. 3) with 3 mJ/pulse of laser excitation. The direct interrogation of the target only shows one Raman peak. Significantly improvement in the returned signal was observed when a small 1" diameter lens (f = 100 mm) was used near the target as FR (as shown in right image). This spectrum is shown in pink color in figure 7. Improvement in the remote Raman signal by FR validated the working principle of this project.

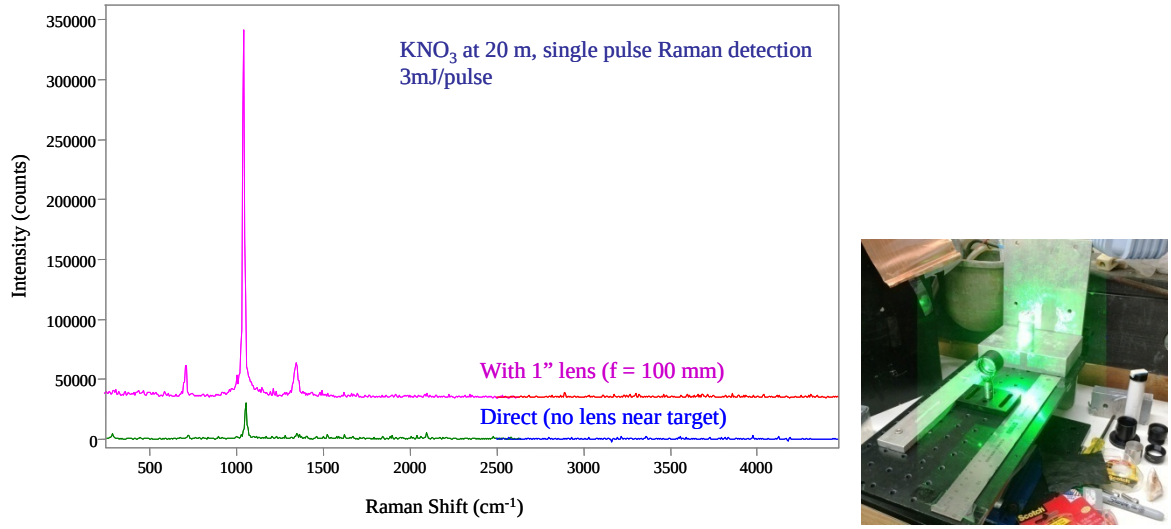

Figure 7. Single pulse standoff Raman detection of KNO_3 at 20 m distance. Laser power 3 mJ/pulse, single pulse integration time. Signal enhancement was observed when a small lens was used near the target as FR (as shown in right image).

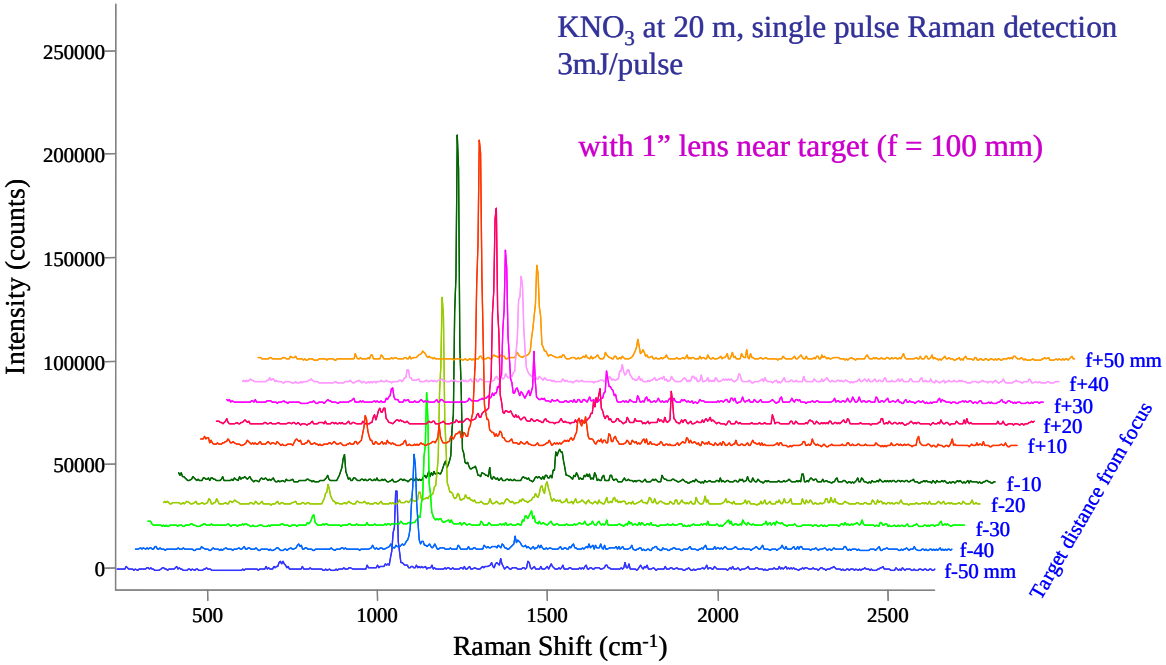

Figure 8. Variation in Raman signal due to defocusing of the lens near the target. Single pulse Raman at 20 m, 3mJ/pulse. Raman signals are observed even when the lens is off focus in both directions by 50 mm, indicating large sampling depth.

For field application, it is important to know how the positioning of the lens affects the signal enhancement. The effect of defocusing the lens near the target was studied by placing the 1" inch diameter lens (f= 100 mm) at various distances from the target (u = 50, 60, 70, 80, 90, 110, 120, 130, 140 150 mm, where u is object distance in mm) and recording single pulse Raman spectra

with 3 mJ/pulse laser energy. This study is useful in estimating the performance of the system if the lens on the distant rover is several centimeters off from its focal length or if the target surface is not uniform and various parts of the targets are located at varying depths. Figure 8 shows that the best signal is observed when the lens is close to its focal point. The system still records good quality Raman spectra of the target even if the lens is in the off focus position in both directions ($u = f \pm \Delta x$, where u is object distance from lens, f is focal length, and Δx is distance away from focal plane).

Similar test was performed at a 40 m distance in the lab using 1 mJ of laser energy. In order to perform the 40 m test a 4" diameter folding mirror was used at the end of lab to reflect the laser towards the target. Figure 9 shows the effect of 1" diameter lens (f = 100 mm) near the target as a function of sample to lens distance.

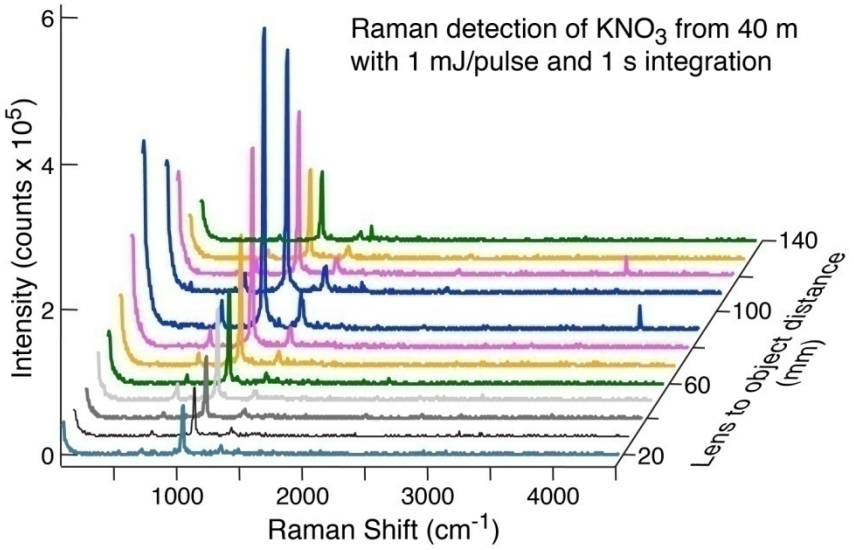

Figure 9. Variation in Raman signal due to defocusing of the lens near the target. Raman spectra at 40 m, 1 mJ/pulse, 1 s. Raman signals are observed even when the lens is off focus in both directions by several centimeters. (1" diameter lens, f = 100 mm)

3.4 ATR-FR system:

Figure 10 shows the picture of ATR-FR system during an outdoor test. In the current project the ATR is an active remote Raman system which sends an active laser pulse and receives the Raman signal generated by the target. The FR is a focusing rover which carries simple optics (lens and a mirror) to direct the laser to the target and collects the generated photons and redirects back to the ATR system. The current ATR-FR system can also work as remote LIBS system. The ATR system can be modify to perform other remote optical detection using absorption, reflection, fluorescence signals. A small frequency-doubled Q-switched Nd:YAG pulsed laser source (Quantel Laser, ultra model, 532 nm, 20 Hz, pulse width 10 ns) excites the distant targets. To acquire the data for this project the laser was operated at low energy of 3 mJ/pulse. An 8x beam expander is used to adjust the size of the laser spot to 50 mm in diameter at 246 m target distance. Two mirrors (M1 and M2) are used to align the laser beam with the optical axis of the telescope making it a coaxial system. The system uses a 500 mm, F8.0 mirror lens (Bower) as a telescope, which has a clear optical collection diameter of 68 mm

and a central obstruction of 32.5 mm in diameter. The scattered light generated by the target was collected by the FR and transmitted towards the remote Raman system. The telescope after receiving the signals focuses onto the 50 micrometer slit of a compact spectrograph of size 10 cm (length) x 8.2 cm (width) x 5.2 cm (height). A 25.4 mm diameter 532 nm long pass filter (Semrock, Inc) is used in the back of the telescope to block out the Rayleigh scattered light. The spectrograph uses a custom HoloPlex grating (Kaiser Optical Systems, Inc.) and is equipped with a custom gated thermo-electrically cooled mini-ICCD detector (Syntronics, Inc.). The spectrograph covers the spectral range from 533 nm to 700 nm which covers the entire Raman spectral range when using a 532 nm laser excitation. The compact spectrograph has pixel resolution of 0.06 nm and spectral resolution of 0.35 nm (FWHM); measured using neon calibration lamp.

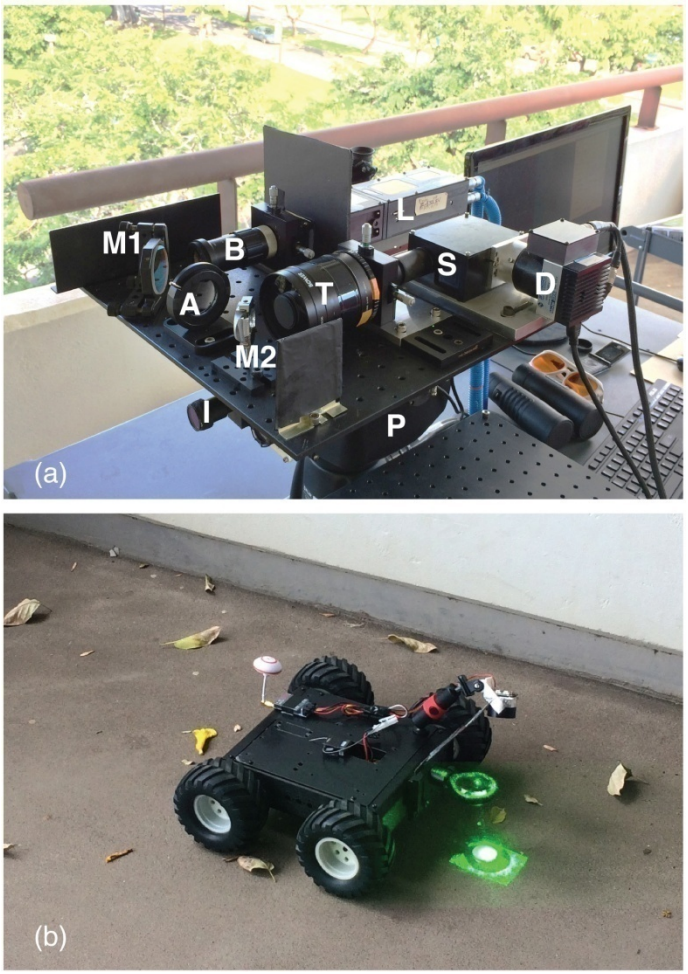

Figure 10. (a) Compact remote Raman+LIBS system developed at the University of Hawaii using 76 mm diameter telescope. L: Nd:YAG pulsed laser 532 nm, B: 8x beam expander, M1: laser mirror, A: aperture, M2: Mirror, T: telescope, S: compact Raman LIBS spectrograph, D: mini-ICCD detector, P: Pan and Tilt scanner, I: imaging camera. (b) Remote controlled car carrying a folding mirror and plano-convex lens for investigating chemicals on the ground.

Figure 10(b) shows the mirror and lens assembly mounted on a remote controlled car to examine targets on the ground. In a simple mode of operation, the operator drives the rover over an area, locates a target of interest on the ground and orients the car using a first-person view (FPV)

video feed so that the mirror is facing the remote Raman+LIBS system. To perform chemical analysis, the car drives over the object, which provides a fixed distance between the lens and the target. For remote LIBS measurements, the lens is placed on the car at a height equal to its focal length. For remote Raman measurements, either the laser power is reduced to avoid LIBS on the target or the lens is placed in a slightly off-focus position. The mirror+lens geometry of FR provides a simple approach to investigate targets which are difficult to detect using direct measurements from long range, such as chemicals on the ground, targets behind a stone or grass, targets floating or submerged in the ocean.

3.5 Remote Raman field tests:

The ATR-FR method was tested outdoor from distances of 120 and 246 meters during daylight. Figure 11 shows outdoor testing of a compact remote Raman system with 3" diameter collection optics and a small spectrograph equipped with a mini-ICCD detector.

Figure11. Compact remote Raman system with a 3" mirror lens as collection optics. Left image shows the field testing of the system with a target distance of 120 m during daylight. Right image shows close up image of the system.

Figure 12 shows detection of ammonium nitrate powder inside a 20 ml glass vial from a distance of 120 m with 3 mJ/pulse of laser power. A small plano-convex focusing lens with 1" diameter and 4" focal length was used near the target (using a field worker as FR) to record remote Raman spectra with single laser pulse, 0.5 s and 5 s integration time. It is shown that all major Raman peaks of ammonium nitrate were detected with 0.5 s integration time. The strong Raman peak at 1044 cm^{-1} corresponding to the symmetric stretching vibration of the nitrate ions NO_3^- in ammonium nitrate is detectable with a single laser pulse excitation with pulse energy of 3 mJ.

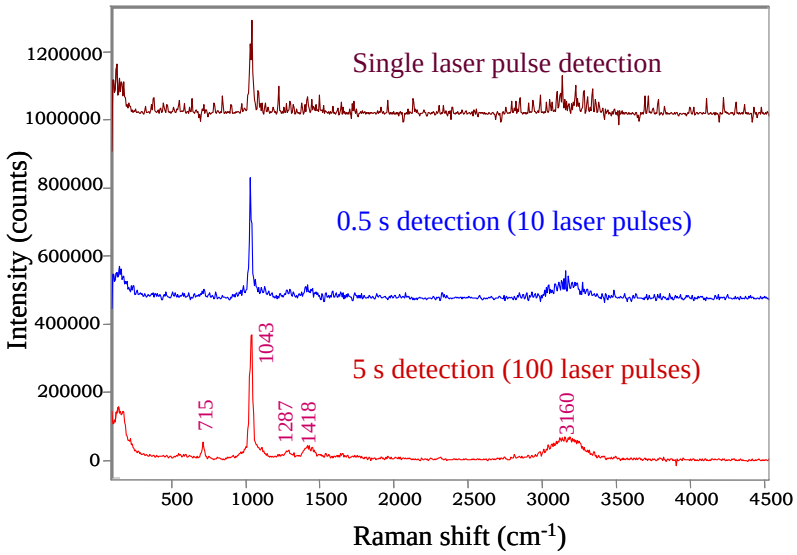

Figure 12. Remote Raman detection of ammonium nitrate from 120 m distance using 3 inch diameter collection optics and 1" diameter focusing lens near the target. Laser power 3 mJ/pulse, 20 Hz. Integration time: single pulse, 0.5 s (10 pulses), and 5 s (100 pulses).

Figure 13. Field test at 246 m target distance. A 6" mirror (shown in top left image) was used at the end of the 128 m long hallway to reflect the laser back to excite the targets placed behind the system as shown in the images on the right.

Field testing of the system was further extended to a distance of 246 m. To achieve the 246 m target distance, a 6" diameter plane mirror was used to reflect the laser beam from the end of the

128 m long hallway as shown in figure 13. The targets were placed behind the system on the ground as shown in figure 13. The system was facing forward towards the mirror. For 246 m tests, a 2" diameter lens with 6" focal length was used as the FR.

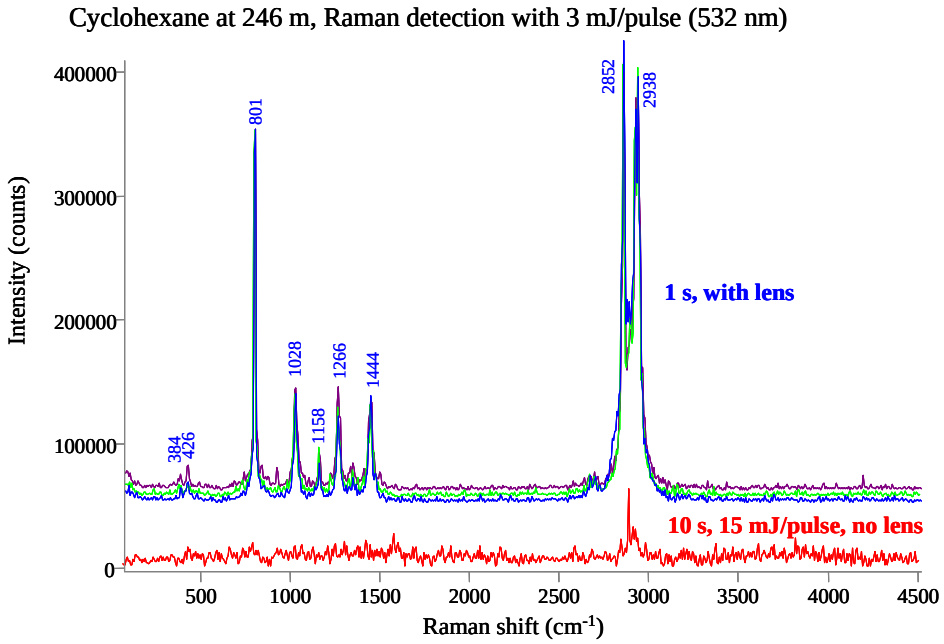

Figure 14. Remote detection of cyclohexane from 246 m distance using the compact remote Raman system. The red plot shows the result of direct detection of a 20 ml cyclohexane vial with 10 s integration time and 15 mJ/pulse of laser energy without the FR. The blue plots were obtained with 3 mJ/pulse and 1 s integration time using a small 2" diameter lens (f = 150 mm) near the target as shown in Figure 13. Three measurements are shown to demonstrate reproducibility (spectra have been vertically shifted for clarity).

Figure 14 shows that with the help of a small 2" diameter lens with 6" focal length Raman signals are significantly enhanced. Figure 14 shows remote Raman spectra of cyclohexane placed inside a 20 ml glass vial from a distance of 246 m. Cyclohexane (C_6H_{12}) is used as a Raman standard (McCreery, 2002) and has a known Raman cross-section of 4.55 x 10^{-30} $cm^2sr^{-1}molecules^{-1}$ with 532 nm laser excitation for the 801 cm^{-1} vibrational mode corresponding to C-C stretch (Acosta-Maeda et al., 2016). The red colored spectrum shows the direct detection of the target using 15 mJ/pulse of laser power and 10 s integration time (= 200 laser pulses). Only a very weak detection of CH Raman bands near 2900 cm^{-1} region is observed. The green-blue colored spectra were obtained with the help of a focusing lens as the FR using low laser pulse energy of 3 mJ/pulse and 1 s integration time. It is shown that all Raman bands of cyclohexane were easily detected from 246 m distance with the help of the FR. This successfully demonstrates the proof of concept proposed under this project. The data shows signal enhancement by a factor of 55000%.

The observed Raman bands of cyclohexane and their corresponding vibrational modes (NIST website) are given in Table 1.

Table 1: Raman fingerprint bands of Cyclohexane (C_6H_6):

Raman Peak (cm^{-1})	**Relative intensity**	**Vibrational mode assignment**
384	weak	CCC deform + CC torsion
426	weak	CCC deform + CC torsion
801	very strong	CC stretch
1028	strong	CC stretch
1158	medium	CH_2 rocking
1266	strong	CH_2 twist
1347	weak	CH_2 wagging
1444	strong	CH_2 scissors
2852	very strong	CH_2 symmetric stretch
2938	very strong	CH_2 antisymmetric stretch

In order to test the long range detection capability of the system without the focusing lens one must use chemical targets which have strong Raman cross-sections and are easy to measure from remote distances using 532 nm laser excitation. Both nitrobenzene and sulfur have strong Raman signals when excited with 532 nm and were used to test the long range remote Raman detection capability. The red colored plot in Figure 15 shows the direct detection of nitrobenzene from 246 m distance using 15 mJ/pulse of laser energy and 10 s integration time. The blue plots showing three measurements with 1 s integration time demonstrate significant enhancement in the Raman signal when a focusing lens is used as the FR near the targets. In the spectra of nitrobenzene the strongest Raman band is observed at 1347 cm^{-1} due to symmetric stretching (ν_s) vibrations of the NO_2 functional group. Other strong Raman peaks in the nitrobenzene spectrum are 853 cm^{-1} (NO_2 sym. bending), 1003 cm^{-1} (C-C-C trigonal bending), 1109 cm^{-1} (C-N stretching+ring breathing), 1588 cm^{-1} (ring stretching) and 3081 cm^{-1} (CH stretch) (Clarkson et al., 2003; Stephenson et al., 1961). A number of organic substances that are rich in nitro (NO_2) groups are often used in explosive devices, such as nitroglycerine, trinitrotoluene (TNT) and triaminotrinitrobenzene (TATB). When combined with strong oxidizers, other nitro-bearing organic substances (e.g., nitrobenzene) also react violently. Raman active symmetric stretching (ν_s) vibrations of the NO_2 functional group are often located between 1300 and 1400 cm^{-1}. A strong Raman peak in this region alarms of the presence of hazardous chemicals with NO_2

group.

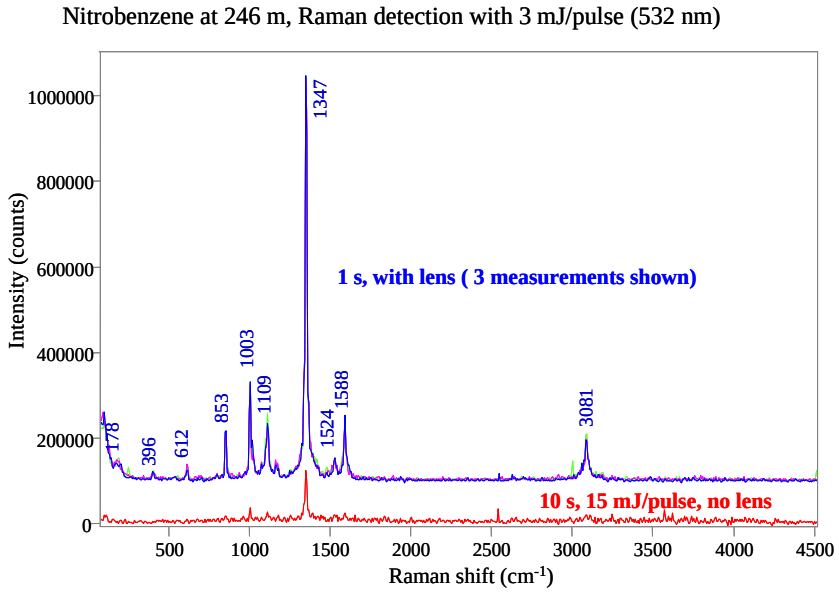

Figure 15. Remote detection of nitrobenzene from 246 m distance using the compact remote Raman system. (Experimental conditions were the same as in Figure 14).

Similar to Figure 15, Figure 16 shows significant enhancement in the Raman signal using a small lens as the FR near a solid sample of sulfur. Sulfur is one of the ingredients in gun powder and can be used as a hazardous material. With 532 nm laser excitation, detection of sulfur from its Raman spectrum is fairly easy because of the very strong Raman signals of elemental sulfur.

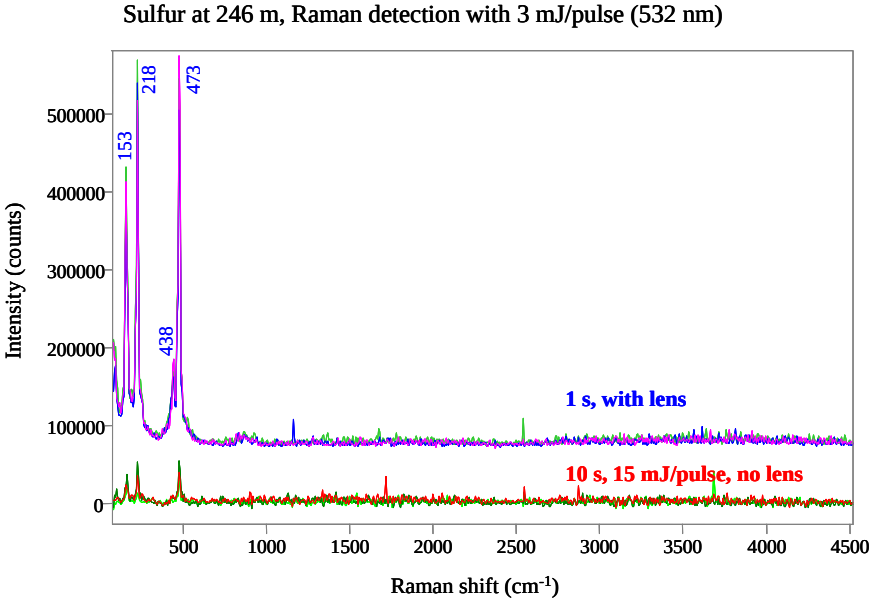

Figure 16. Remote detection of sulfur from 246 m distance using the compact remote Raman system. (Experimental conditions were the same as in Figure 14).

In Figure 16, the diagnostic Raman lines of elemental sulfur are clearly visible at 246 m distance, even in the direct remote Raman measurement. At room temperature, crystalline sulfur exists as cyclic crown-shaped S_8 molecules. There are eleven fundamental vibrational modes, and all of them are Raman active (Anderson and Loh, 1969). Three of the eleven fundamental modes give rise to intense, sharp Raman peaks (Figure 16) at 153, 218 and 473 cm^{-1}. These peaks are attributed to the doubly degenerate bending (ν_δ), symmetric bending (ν_2) and symmetric stretching (ν_1) vibrations of the cyclic molecule, respectively (Harvey and Butler, 1986, Gautier and Debeau, 1974, Pasteris et al., 2001).

Figure 17 demonstrate that with the help of a focusing lens, good quality remote Raman spectra can be obtained within a second during daytime. Figure 17 shows detection of benzene inside a 20 ml glass vial from 246 m distance with single pulse, 10 pulses and 20 pulses integration times and using low laser pulse energy of 3 mJ/pulse. A 2" diameter lens with 150 mm focal length was used as the FR.

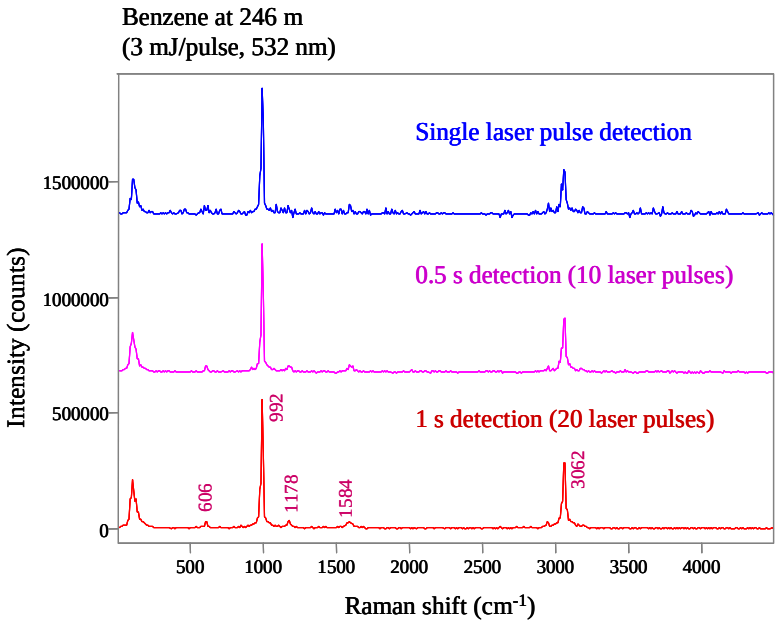

Figure 17. Remote Raman detection of benzene from 246 m distance using 3 mJ/pulse, 532 nm and 2" diameter focusing lens (f = 150 mm). Integration times: single pulse, 0.5 s, and 1 s.

The ability to perform remote Raman spectroscopy from 246 m distance using low laser pulse energy is a significant achievement in the field of remote chemical detection using fingerprint Raman signals. Raman signals are very weak and on average only one Raman photon is produced for every 10 million laser photons used for excitation. Despite the very low signal strength, a significant advantage of Raman spectroscopy is that it provides a very high level of confidence in chemical detection. Raman spectroscopy is capable of distinguishing between very similar chemicals. As an example, remote Raman spectra of benzene, ethyl-benzene and nitro-benzene from a distance of 246 m with 1 s integration time is given in Figure 18.

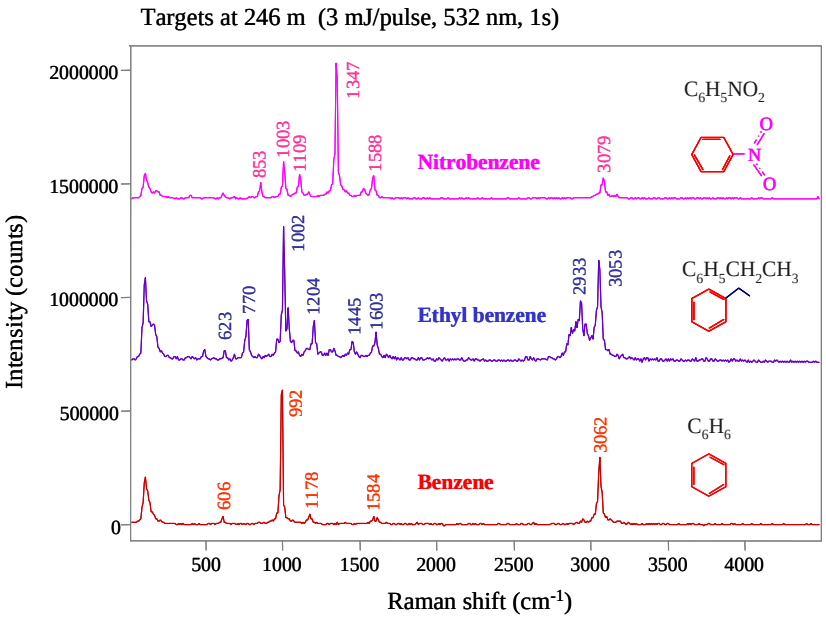

Figure 18. Remote Raman detection of benzene, ethyl-benzene and nitro-benzene from 246 m distance with 1 s integration time using 3 mJ/pulse, 532 nm and 2" diameter focusing lens (f = 150 mm).

Figure 19 shows detection of sulfuric acid, nitric acid and water with 1 s integration time and low laser power from 246 m distance. The capability to identify hazardous liquids through glass and plastic bottles will be helpful for screening water bottles at airports and other check points.

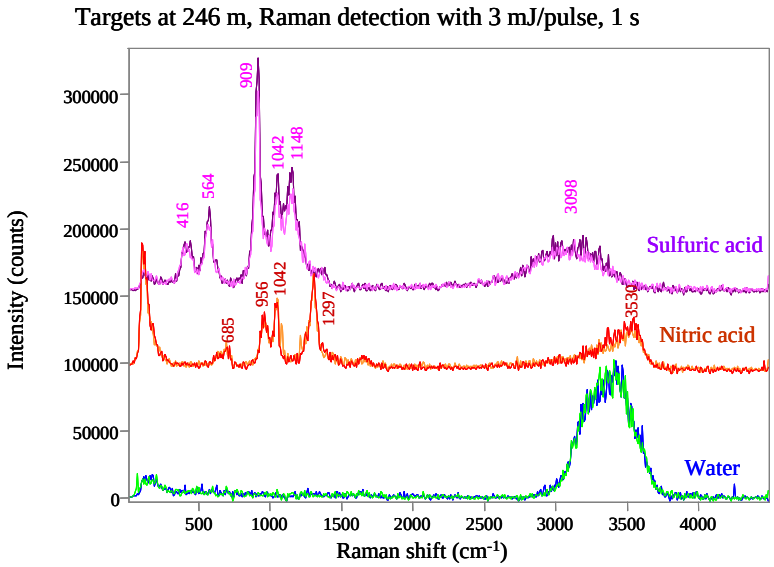

Figure 19. Remote Raman detection of sulfuric acid, nitric acid and water from 246 m distance with 1 s integration time using 3 mJ/pulse, 532 nm and 2" diameter focusing lens (f = 150 mm). Liquid samples were measured through sealed 20 ml glass vials. Two measurements are shown for each sample to demonstrate reproducibility.

In the spectra of sulfuric acid, a strong peak near 909 cm^{-1} is assigned to antisymmetric stretching of HO–S–OH. The other Raman bands observed near 1042 and 1148 cm^{-1} are due to symmetric stretch of O=S–OH and O=S=O (Fraenkel, 2015). In the spectra of nitric acid, Raman peaks are observed at 685 cm^{-1} (NO_2 bending scis.), 956 cm^{-1} (N-O stretch), 1042 cm^{-1} (NO_3 sym stretch) 1297 cm^{-1} (NO_2 sym stretch) (Ratcliffe and Irish, 1985).

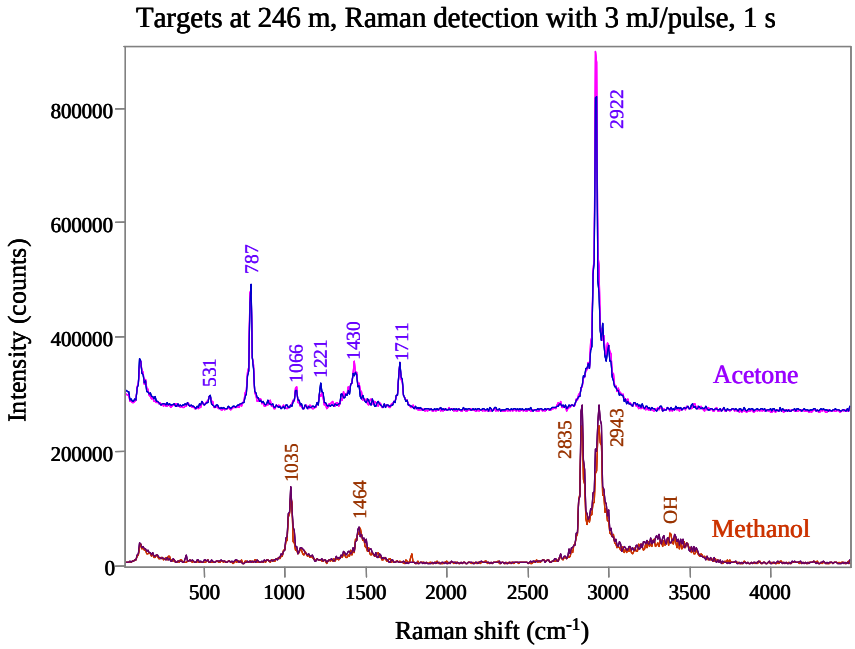

Figure 20. Remote Raman detection of acetone and methanol from 246 m distance with 1 s integration time using 3 mJ/pulse, 532 nm and 2" diameter focusing lens (f = 150 mm). Liquid samples were measured through sealed 20 ml glass vials. Two measurements are shown to demonstrate reproducibility.

Figure 20 shows the remote Raman spectra of acetone and methanol through sealed 20 ml glass vials from 246 m distance and with 1 s integration time using 3 mJ/pulse of laser energy. All fingerprint Raman bands of these organic solvents were easily detected. In the spectrum of methanol, two of the most intense Raman peaks are from the symmetric stretching (ν_s) and Fermi-resonance enhanced bending overtone vibrations of the methyl (CH_3) group: 2835 and 2943 cm^{-1}, respectively (Mammone et al., 1980, Furic et al., 1993, Misra et al., 2007). A medium intensity peak attributed to stretching vibrations of the C-O bond is found at 1035 cm^{-1}. In addition, a very broad, weak band extending from 3100 to 3600 cm^{-1} can be found in various kinds of alcohols, attributed to the hydroxyl (OH) stretching vibrations. The most intense Raman peak of acetone is located at 2922 cm^{-1}, also attributed to the ν_s vibrations of the methyl groups. Another strong peak at 787 cm^{-1} is attributed to the C-C stretching vibrations. Furthermore, a signature peak from the C=O stretching vibrations can be found in all carbonyl compounds, which is located between 1600 and 1800 cm^{-1} (1711 cm^{-1} in acetone) (Dellepiane et al., 1968, Misra et al., 2007).

Figure 21 shows the remote Raman detection of ammonium nitrate (NH_4NO_3) and potassium nitrate (KNO_3) from 246 m distance with 1 s integration time. The data were collected using a 2" diameter focusing lens (f = 150 mm) as the FR as shown in Figure 13. Solid targets were placed at closer distance than the focal length of the lens in order to avoid LIBS on the targets. The distance between the focusing lens and the targets was 145 mm. Under this condition, good quality Raman spectra could be measured from all solids without causing LIBS.

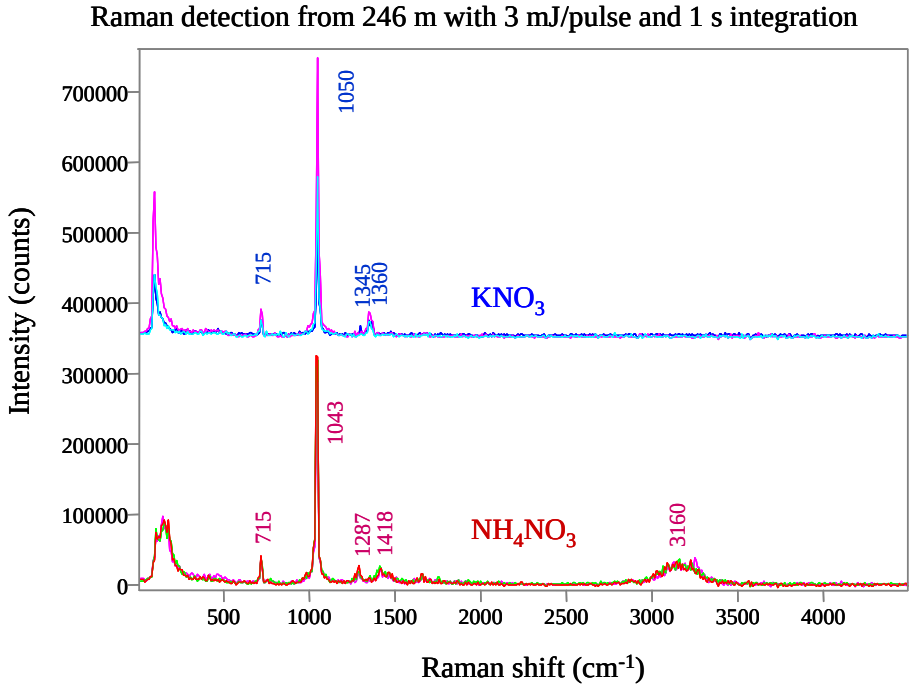

Figure 21. Remote Raman detection of potassium nitrate and ammonium nitrate from 246 m distance with 1 s integration time using 3 mJ/pulse, 532 nm and 2" diameter focusing lens (f = 150 mm). Solid powder samples were measured through sealed 20 ml glass vials. Three measurements with 1 s integration times are shown for each chemical to demonstrate reproducibility.

All major Raman bands necessary for the positive identification of ammonium nitrate are clearly observed. Ammonium nitrate is often used in the production of homemade explosive materials due to its easy accessibility in the agriculture industry as a nitrogen-rich fertilizer. In the spectrum of NH_4NO_3, the intense Raman peak at 1044 cm^{-1} is attributed to the symmetric stretching (ν_1) vibration of the nitrate (NO_3^-) ion. The Raman peaks at 715 cm^{-1} and between 50 and 250 cm^{-1} are, respectively, the in-plane bending (ν_4) vibrations of the NO_3^- ion, and the lattice (translational and rotational) vibrations of the NO_3^- and NH_4^+ ions. (Harju, 1993; Akiyama et al., 1981).

The symmetric stretching (ν_1) vibrations of the nitrate (NO_3^-) ion in the KNO_3 are observed at 1052 cm^{-1}. NH_4NO_3 can also be easily distinguished from KNO_3 by the presence of a broad Raman band in the high-frequency (high Raman shift) region near 3137 cm^{-1} which is due to the symmetric stretching vibration of NH_4^+ ion (Misra et al., 2012). The asymmetric stretching mode of the ammonium ion gives a Raman band near 3225 cm^{-1}, which contributes to the broadness of the Raman band in the high frequency region.

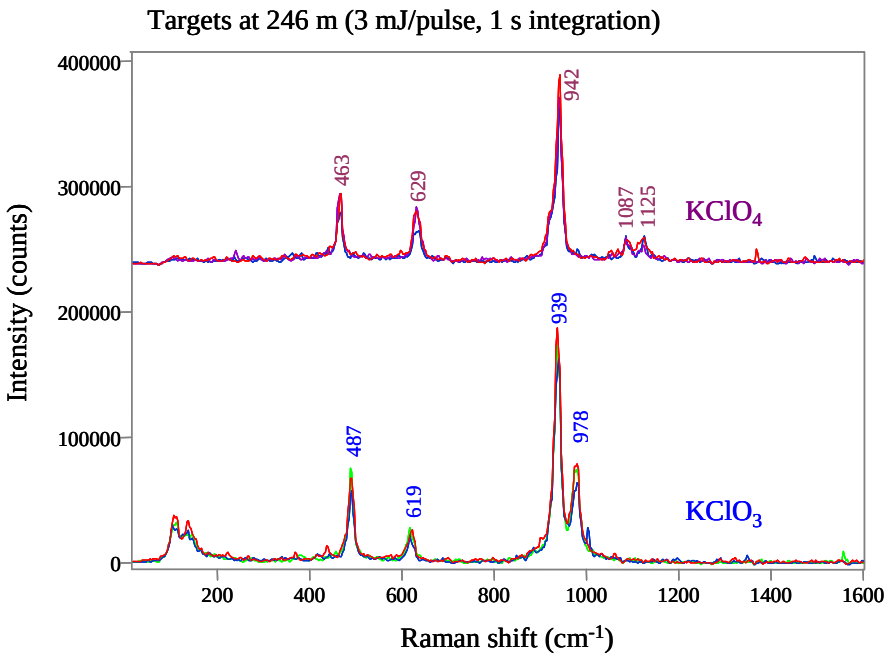

Figure 22. Remote Raman detection of potassium perchlorate and potassium chlorate from 246 m distance with 1 s integration time. Experimental conditions were the same as in Figure 21.

Figure 22 shows remote Raman spectra of $KClO_4$ and $KClO_3$ under the same experimental conditions as in Figure 21. In the spectrum of $KClO_4$, the intense Raman peak at 942 cm^{-1} is attributed to the symmetric stretching (ν_1) vibration of the chlorate (ClO_4^-) ion, and the shoulder peak at 924 cm^{-1} to the first overtone of the symmetric bending (ν_2) vibration of the ClO_4^- ion. The signal intensity of the latter is enhanced by the Fermi resonance effect (Bini et al., 1990). Fermi resonance is observed in the Raman spectrum when the vibrational frequency of an overtone mode is in the vicinity of a symmetric fundamental mode (the Raman frequency of the ν_2 fundamental mode of ClO_4^- is 463 cm^{-1}). Other Raman peaks of the ClO_4^- ion are 629 cm^{-1}, attributed to the antisymmetric bending (ν_4) mode, and at 1087 and 1125 cm^{-1}, attributed to the antisymmetric stretching (ν_3) vibrational modes (Lutz et al., 1983; Troupry et al., 1983). In the $KClO_3$ Raman spectra, the symmetric stretching vibration of chlorate ion is observed at 939 cm^{-1}. In the chlorate, the Raman bands corresponding to the υ3 and υ4 vibrational modes of the ClO^-_3 appear at 489 and 619 cm^{-1} (Acosta-Maeda et al, 2016 b).

3.6 Remote LIBS field tests:

ATR-FR system was also used to test the remote LIBS capability. For the remote LIBS data, the position of small lens near the target is adjusted so that it is exactly at the focal point. When using a person to hold the lens near the target, the LIBS signals are optimized by listening to the loud sound of LIBS shots (shock waves) and adjusting the lens position. Under this project, it was found that it is easier to perform remote LIBS than remote Raman. Figure 23 shows the remote LIBS spectra of barite ($BaSO_4$) and dolomite ($CaMg(CO_3)_2$) from a distance of 246 m using single laser pulse of energy 3 mJ/pulse. In the barite LIBS spectra all spectral lines

correspond to Ba. In the dolomite spectra most of the atomic spectral lines corresponding to Ca. Mg is observed at 552.84 nm and a Na doublet is observed at 589.0 and 589.59 nm.

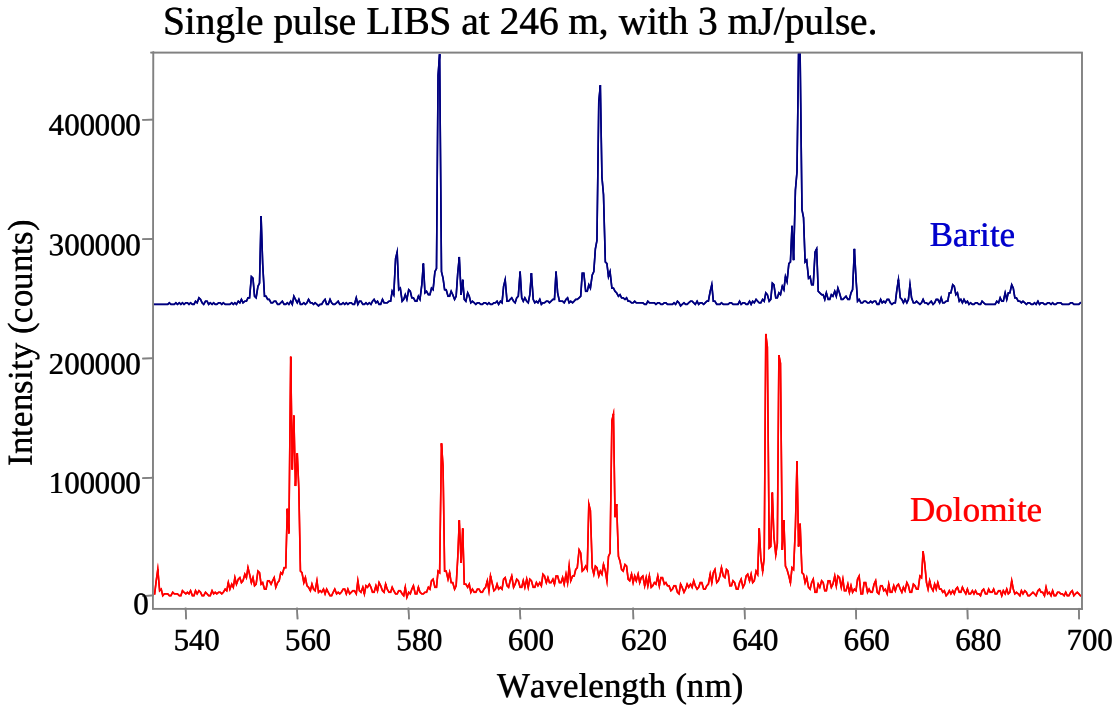

Figure 23. Single pulse remote LIBS spectra of barite and dolomite mineral rocks from 246 m distance using 3 mJ/pulse of 532 nm pulsed laser and 2" diameter focusing lens (f = 150 mm) as the FR.

Figure 24 compares the remote LIBS spectra of barite with single laser pulse and with 1 s integration time (equivalent to 20 laser pulse interrogation) from a distance of 246 m. It is shown that significant improvement in the LIBS signal is obtained when signal is accumulated for just one second. The 1 s LIBS spectra also shows decrease in the Na doublets observed at ~589 nm in comparison to single pulse spectrum, indicating that salt deposit is only limited to the surface of the target.

The ability to conduct remote LIBS from a target distance of 246 m with low laser pulse energy of only 3 mJ/pulse by employing the ATR-FR method is significant achievement in the field of remote LIBS spectroscopy. This method has not only broken the world record for conducting LIBS at long distances, but also uses very low laser pulse energy in comparison to currently used remote LIBS systems.

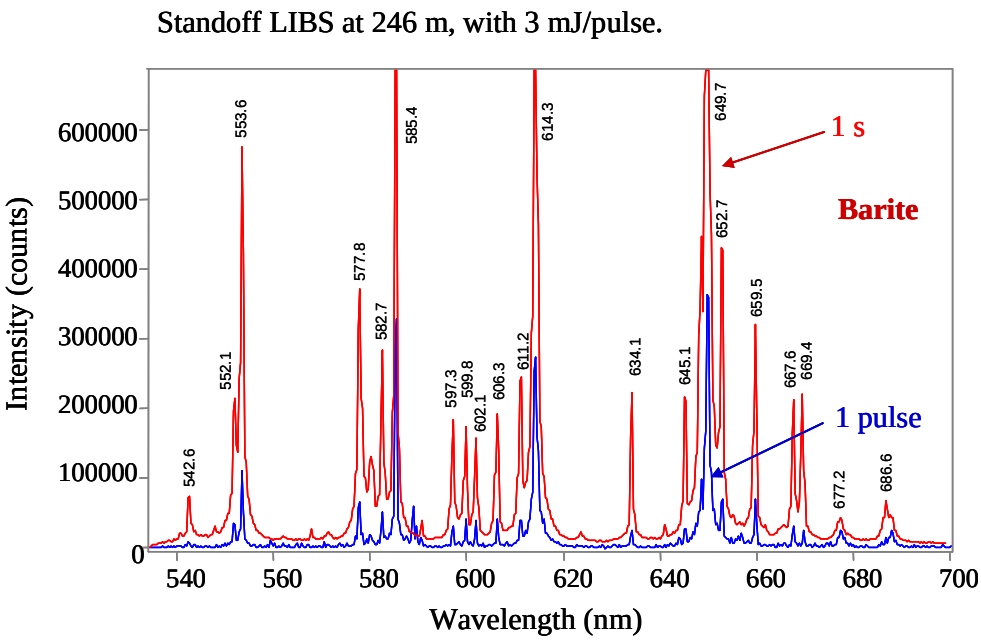

Figure 24. Remote LIBS spectra of barite rock from 246 m distance with low laser pulse energy of 3 mJ/pulse. The spectrum shown in red plot integrated for 1 s (= 20 laser pulses interrogation) shows significant improvement in S/N ratio in comparison to single pulse LIBS spectrum (shown in blue).

Figure 25. Comparison of the system size and detection range. On left is the remote LIBS system from Univ. of Malaga, Spain, with 50 m range using 1600 mJ/pulse laser energy at 1064 nm (Laserna et al., 2007). On the right is the ATR-FR method (Univ. of Hawaii) testing successful remote LIBS at 246 m with single laser pulse of 3 mJ/pulse (532 nm) and small collection optics.

With previous funding from ONR, the University of Hawaii has developed a combined remote Raman+LIBS system using an 8" diameter telescope. The system using laser pulse energy of 100 mJ/pulse at 532 nm was able to successfully conduct remote LIBS tests at 50 m distance using a large 10x beam expander. The conventional remote LIBS systems are limited in range due to difficulty in focusing the laser at longer target distance to achieve high optical energy

density required to breakdown target molecules. To best of our knowledge, Dr. Javier Laserna's group in Spain (Univ. of Malaga) holds the world record for conducting LIBS on few selected targets which are easy for LIBS excitation at the distance of 130 m using a large system and using pulsed laser with 350 mJ/pulse at 1064 nm (Lopez-Moreno et al., 2006). Their newer system uses 1600 mJ/pulse at 1064 nm and is designed to perform standoff LIBS on regular targets at distance of 50 m (Laserna et al., 2007). Figure 25 shows the picture of the Spanish remote LIBS system (left image). The right image shows the work performed under this project where a small system using low laser pulse energy (3 mJ/pulse) could easily do LIBS at much longer target distance of 246 m.

3.7 Field testing with ground focusing rover:

Figure 26. Field testing of remote control car as FR. (a) Shows the remote-control car equipped with mirror and lens assembly to look for targets on the ground, a live video feed showing the lens and the ground and a remote controller. The target shown in (d) is located at the far end of the corridor at distance of 125 m. The ground FR was driven from the system to the target (images (b) and (c)) and rotated to align the mirrors to face the system for laser excitation.

A remotely controlled car was developed with first-person view (FPV) video feed as the ground focusing rover. In Figure 26, image (a) shows the remote controlled car equipped with a flat mirror and a 2" diameter lens to look for targets on the floor. A FPV camera is mounted on the top of the lens. The video feed from the car shows the lens and the ground (as shown in image (a)). The remote controlled car runs on 12 V battery pack and was used for field testing to find a target 125 m away on the other side of the hallway. Images (b) and (c) show the operator driving the car towards the target. Once the car reaches the target, operator tries to turn it around so that the mirror is facing towards the ATR system and video feed from the car

shows the target. Operator then tries to move the car so that lens is over the target. At this point the ATR system locates the ground FR and fire the laser to the mirror. For this field test, the laser beam was expanded, so that part of the laser is falling on the mirror attached to the car. Figure 27 shows results of three measurements of ammonium nitrate sample at the distance of 125 m with 1 s integration time. The variation in the return signal is due to the difference in the mirror angle and amount of laser beam falling over the mirror during three driving tests. The three tests were conducted by the car making three separate attempts to locate the target and aligning itself.

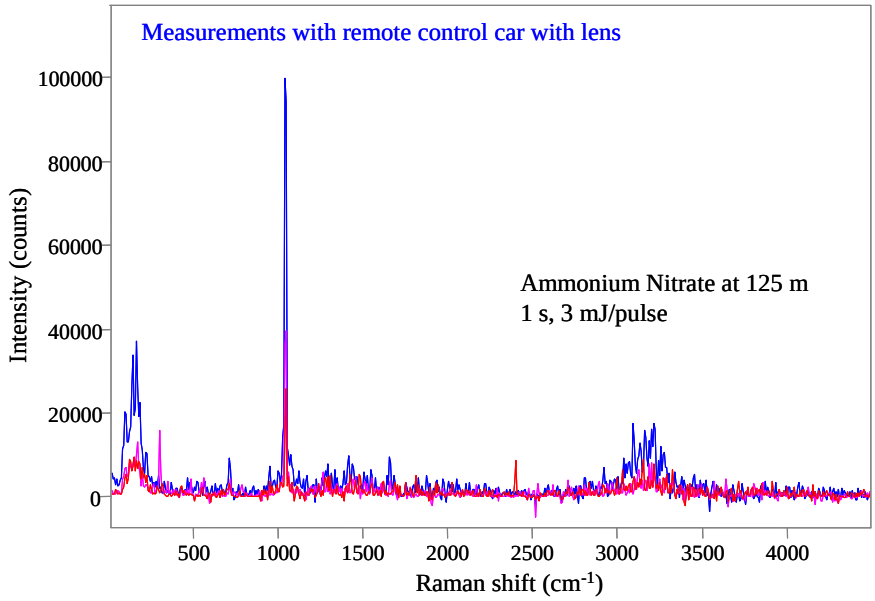

Figure 27. Results of three driving tests of remote controlled car over a target placed at 125 m distance on ground (as shown in Figure 20). Three measurements with 1 s integration time are shown. The variation in the Raman signals is due to difference in the mirror angle and amount of laser beam falling over the mirror during three driving tests.

Figure 28 shows result of another field test data obtained from 125 m distance using the remote controlled car to look for a target placed on the ground as shown in Figure 26(d). Remote Raman spectra were measured with 3 mJ/pulse energy. Two measurements are shown with 1 s integration time using the car. The two tests were conducted by the car making two separate attempts to locate the target and aligning itself. The Raman spectra confirm the target to be calcium carbonate. The direct measurements of the target show no Raman signal. Direct measurements were made by holding the target vertically and using the 3 mJ/pulse energy for excitation.

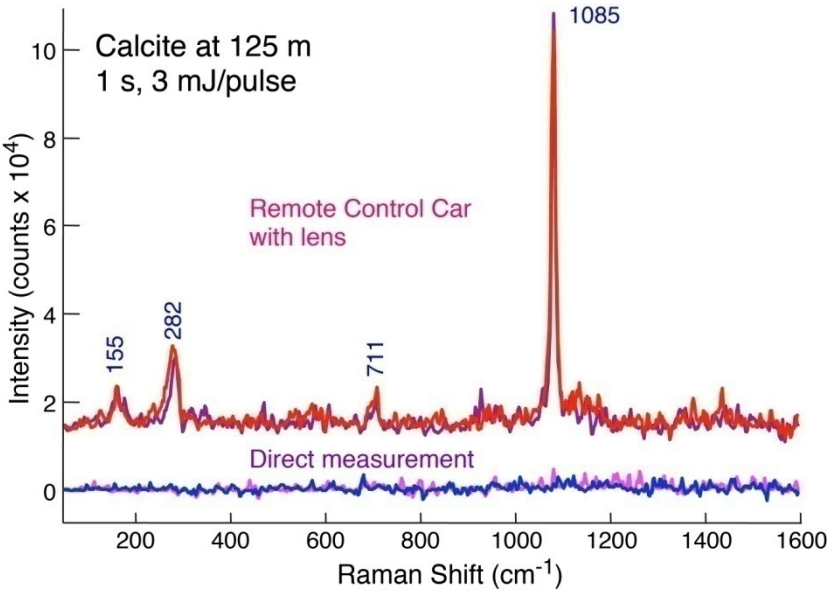

Figure 28. Results of two driving tests of remote controlled car over a target placed at 125 m distance on ground. The Raman measurements with 1 s integration time are shown. For direct measurements, the target was held vertically.

3.8 Research effort with drone as focusing rover:

Under this project we also investigated the possibility of using a drone as a focusing rover. For this task, we tested several method s for actively tracking a drone and firing the laser to the mirror/lens assembly attached to the drone. Initially, a computer vision method (based on cross correlation) was used to detect the location of the drone and controls the pan-tilt so that the remote Raman system points at the drone target. Figure 29 shows an image of the Matlab control GUI with options to do various tasks. The first task is to view both the narrow and wide view simultaneously. The 2nd-4th options are to point the laser at a specific object by clicking on the object in one of three live camera images (wide, narrow (zoomed), very narrow with a 500 mm fl telescope). The ability to carry out this process with different camera zoom factors provides diverse pointing control (within the stepping resolution of the pan-tilt motors). The 5th GUI option allows the user to define a template image (a cropped region of target) which will be tracked in future images. By selecting the drone to be within the cropped image, the system will track the position of the drone in future images, and actively point the laser at the drone. Matlab software to track the selected template and to actively point the pan-tilt laser system was developed.

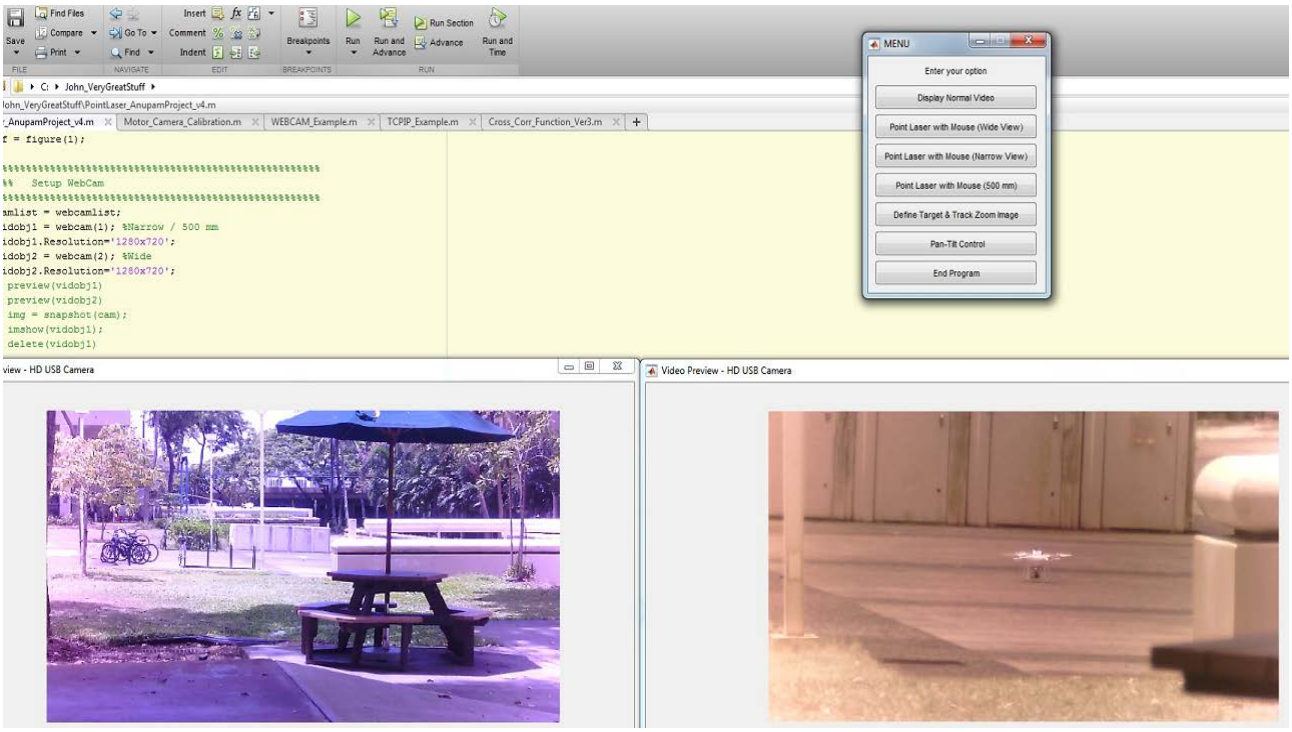

Figure 29. Computer screen shot showing the user GUI (top right) and the live wide and narrow (zoomed) camera images.

Figure 30 shows an example of the first image a user would see before defining the target to be tracked. The red circle, in the center of the image, defines the location of the laser. A target is defined by drawing a box. As an example, the white paper circle seen on the right side was selected as the target. The control software pointed the laser pan-tilt system at the new location of the white circle as shown in the middle image. The target was moved in the bottom image and the system successfully tracked the target providing live images. This example shows that when the target is well defined in the template image then it is possible to track the target and to automatically point the laser pan-tilt system correctly.

Figure 30. The top figure shows the image before the user has selected the target template region. The red circle in the center of the image is the position of the laser. The target is the white circle seen on the right of the image. After user defines the white circle as the target, the system automatically follows the target as shown in middle and bottom figures.

Figure 31 show a case where tracking tests were carried outdoors in the daylight. Here the drone was selected in the template region of the narrow field of view images. The drone was flown and its position was tracked with the imaging software and the laser pan-tilt system actively pointed at the drone. The distance from the system to the drone was approximately 60 m.

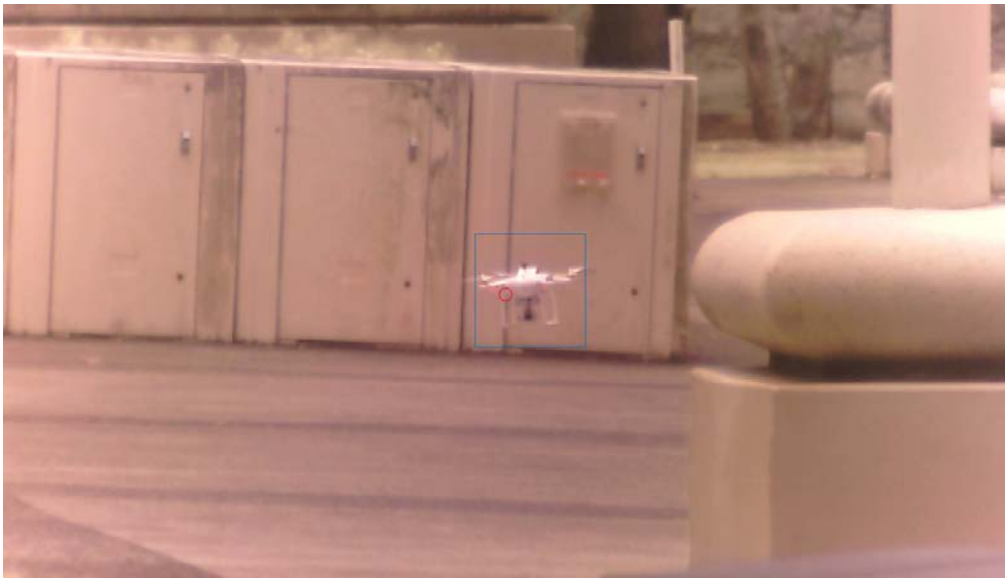

Figure 31. Screen shot image taken from the control software showing the control software tracking the drone (blue box) and the pan-tilt attempting to keep up (red circle).

The outdoor tests carried out to date found that the procedure is promising but not ideal. The drone tracking shown in figure 31 worked while the white background was present but when the drone rose above the white background the correlation decreased and the drone was no longer tracked. The active tracking also failed when the image of the drone was lost due to either drone disappearing behind objects or because of people walking and crossing-over the line of sight.

A different tracking method was tested which consisted of using a 940 nm NIR led light source mounted on the drone. The camera mounted on the remote Raman pan-tilt system was modified by removing the NIR blocking filter and installing a 940 nm band pass filter.

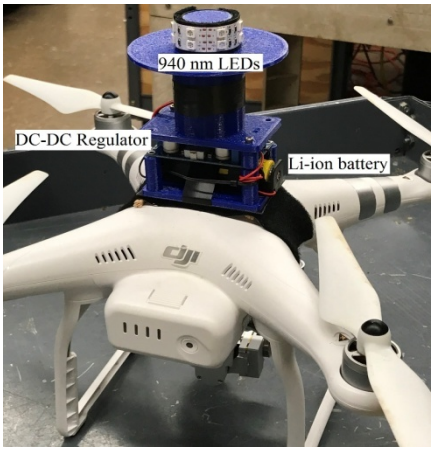

Figure 32: DJI drone with 940 nm IR LED and custom regulated power supply. The power supply provides steady 8V to LED for more than 1 hour.

Figure 32 shows a picture of the 940 nm light system built for mounting on the drone. The components consist of a Li-ion battery (3.6 – 4.2 volts), a dc-dc voltage regulator, a 3D printed

assembly, and a bank of 940 nm led lights. The dc-dc voltage regulator is used to provide a steady 8 volts even as the battery voltage decreases with time. Tests were carried out and system provided NIR light for over an hour with no problem. The led lights are located in an elevated location to be above the drone propellers. The goal of this design was to reduce the possibility of reflections off the propellers. During laboratory tests it was sometimes found that light reflections could affect the position detection algorithm. The structure of the support was 3D printed PETG which was made hollow to reduce weight. Field tests of the DJI drone, with the LED system installed, found that it did not affect the flight in any noticeable way (Figure 33).

Figure 33: Outdoor testing of DJI drone with 940 nm LED's.

In order to reduce ambient light the camera uses a 940 nm band pass filter. Various field tests have found that even with this filter the camera system reading too much background light. Several steps were taken to reduce the background light including the use of a moderate size pin hole in front of the camera and by reducing the integration time in software. With these two additional constraints, the background light was reasonable and could be controlled by adjusting the camera integration time. Figure 34 and 35 show two computer screen shot images with the camera integration time set to different settings. These figures show both the wide and narrow field of view camera images as well as the control GUI (graphic user interface).

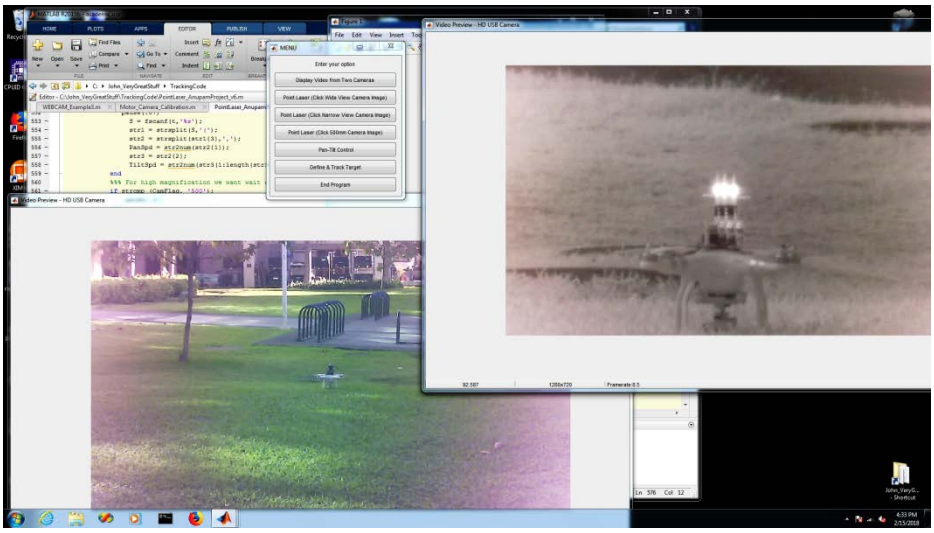

Figure 34: Computer screen shot showing the live video from the wide and narrow field of view cameras. The narrow field of view camera has the 940 nm band pass filter and looks for bright IR signal.

Tracking tests were carried out with the drone led system in the field of view of the narrow image. It was found that the tracking was working well but had a slow reaction time. If the drone moved rapidly then it had the possibility of leaving the view of the narrow field of view camera and tracking failed. The tests described here were with the drone at a distance of ~20 m. This is rather close and this tracking loss would not occur at greater distance (100 m). In any case it would be desirable that the tracking work well at any distance.

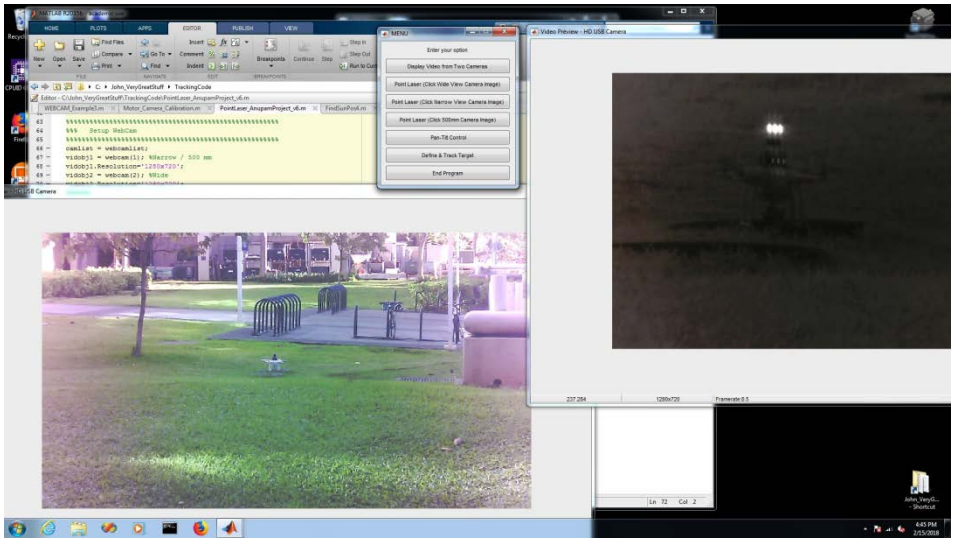

Figure 35: Computer screen shot (similar to Fig 34). By adjusting the camera setting on narrow field of view camera, it is possible to block out the background light and only see the 940 nm LED's for tracking the drone.

Several steps were tested to improve the tracking performance of the system. The first change was to use a wider field of view on the NIR camera. A 50 mm focal length lens was changed to a 16 mm focal length lens. This provided a wider view for tracking the 940 nm led on the drone. The new camera-lens combination was calibrated (viewing angle of each pixel) and tested. This design leaves the wide field of view camera for scene imaging and uses the moderately narrow field of view camera for tracking the 940 nm LED on the drone. The Matlab codes were updated to improve the speed of tracking. This resulted in significantly faster and more reliable camera control code. The LED tracking algorithm is based on getting the average position of the brightest pixels in the image. This process involves sorting the pixels based on brightness levels and selecting the top 0.01% brightness levels. For a 1 Mega pixel image, this corresponds to 100 pixels. If the drone is close then the LED appears large in the image and all the selected brightest pixels correspond to the LED. If the drone is further, the LED will occupy less than 100 pixels and the algorithm will calculate the average position of brightest pixels, which include the LED as well as other bright objects in the image. This can cause an error in tracking and pointing. Tests were carried out and it was observed that most of the time the tracking was correct but on occasion a car (with sun reflection) passed by in the background, causing temporary errors in the tracking process.

Improvements to the tracking software were implemented. Rather than searching the whole image for bright pixels (corresponding to the NIR led) a smaller search area image was defined and used for this purpose. The search area image was a cropped from the larger image centered over the location of the bright spot in the last large image collected. An example of this small search area is shown in Figure 36. There are several advantages to only searching a smaller section of the large image. First, if a bright spot appears on the edge of the image (a moving car, etc…) then that part of the image is not searched and it does not cause tracking errors. Secondly, if the vision to the NIR led is blocked (someone walked in front) then future searches are only carried out in the region where the NIR led was last seen and not over the entire large image. Thirdly, searching a smaller portion of the image speeds up the algorithm. The algorithm is also setup so that if the NIR led is not visible (no pixels greater than 50 counts) then the pan-tilt is not moved and the software continues searching in the same location. The software also allows the user to enter a character ("n") to stop the loop and define a new search location within the image. This is useful in the event the system tracks an incorrect target or the NIR led exit the small search area. Alternatively the user can enter a "q" character to stop active tracking and point to a new location with other options in the code. The tracking algorithm consists of the following sequence,

1) an image is captured from the narrow field of view camera (NIR camera),
2) a search image (centered over the last target position) is cropped from the larger captured image,
3) the position of the bright spot is located in the search area image,
4) if the bright spot is brighter than 50 counts then it is considered valid,
5) the position of the bright spot is calculated in the larger NIR camera image,
6) the distance the motor needs to move is calculated in camera pixels and then motor steps,
7) commands are sent to the stepper motor and it moves the given number of steps,
8) the process is repeated above.

The software described above has been optimized and is working well. At this time the algorithm has been speed up to ~4 cycles per second (each cycle includes collecting an image,

processing it, and sending commands to the motor).

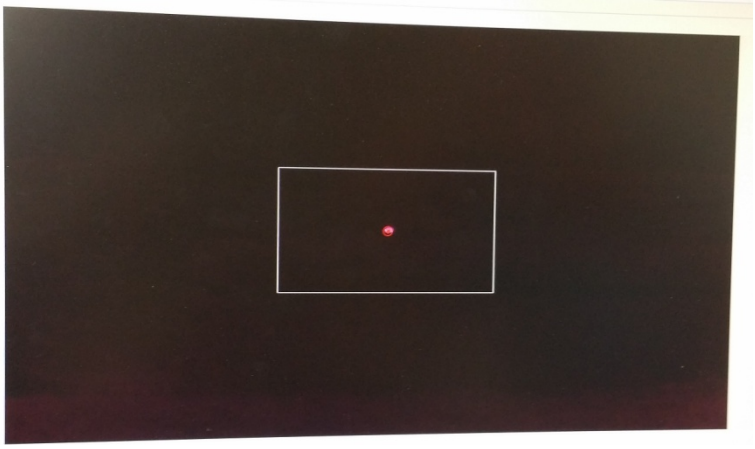

Fig. 36. Image showing the larger image and the rectangular region where a smaller image is cropped. The cropped image is searched for bright targets. In this case the system laser (shown as a circle) is close to the bright spot (* symbol) as expected for proper tracking.

Efforts were made to conduct field tests on the drone+System for tracking of the drone and remote chemical detection using the system. Figure 37 shows the outdoor test area at the University of Hawaii. Although we plan to perform remote Raman detection at low laser power of 3 mJ/pulse with beam diameter of 50 mm, it is still considered not eye safe. In order to perform safe outdoor testing with a class IV pulsed laser, so that there is no risk of accidentally hitting someone with the laser, we moved the system to 2nd floor of our building. The idea was to interrogate targets which are placed at a height above people's eye level, so that no person could be in the direct line of sight. For elevating the target, a large plastic drum was used (shows as white drum in the middle of the grass field). A large tarp was mounted on the wall of the building shown on far side for eye protection. In addition, guards were placed near the area to look out for possible human traffic and to halt the field test.

Figure 37. Outdoor testing of the system. For eye safety, the system was placed on the second floor and targets were placed on a white drum shown on the far end of the image. The line of sight was several feet above normal human height except near the target, where guards were placed to stop people to walk in the laser beam.

Unfortunately, this test site did not work out as planned. The operator flew the drone from the system end and was able to locate the targets from the video feed from the drone. As the operator was trying to land the drone on the target (as shown in the right image), the drone suddenly stopped hovering, drifted with the wind and crashed in the tree within a few seconds with no time to react. Similar DJI drone mishaps have been reported by several people on the web where drone lost radio control and took off at full speed or lost GPS positioning. The crash destroyed the lens mounting assembly too. We now have a newer drone which is equipped with additional optical sensors to avoid crashing. We are now searching for an open secure area where field tests could be performed using the pulsed 532 nm laser (not-eye-safe). We will report theses data to ONR as soon as possible.

4. Summary:

Under this ONR project, we developed a simple two-component system to conduct long range chemical detection using remote Raman and LIBS spectroscopy. The first component is a

small remote Raman+LIBS system and the second is a simple lens and mirror assembly, which is used near a distant target by a field worker, remote controlled vehicle, or UAV. Using this approach we obtained good quality remote Raman measurements on various targets from a distance of 246 m using 532 nm pulse laser with 3 mJ/pulse energy and 1 s integration time. Remote LIBS measurements at 246 m distance could be easily obtained with single laser pulse excitation of 3 mJ.

There are several advantages of two component system over a single system. Adding a simple lens near the target increases both the system's detection range and sensitivity. The data presented here suggest that both Raman and LIBS capabilities are significantly improved at long working distances. The method is especially of interest to use of human in field operations where chemical analysis of field targets can be done by simply carrying simple optics without carrying the bulky instruments and without collecting samples. The method is also applicable to analyze targets using UAV which are difficult to access or hazardous, such as floating or submerge debris in the ocean, mineral layers on a steep cliff, hazardous chemical spill, toxic fumes and gas leaks, active lava flow, deep caves, methane icebergs etc.

This method could be used on future projects using UAVs for remote chemical detection. By simply attaching a mirror and small lens to the UAV, it is possible to analyze distant minerals on the ground by using a small remote Raman and LIBS system housed away from the UAV and near the operator. The method also provides a safer remote LIBS operation in comparison to direct interrogation of targets using high pulse laser energy.

This research work demonstrates significant improvements in the remote Raman and LIBS signals for analyzing targets at hundreds of meters using low laser power and short integration time. The methodology is simple and expected to further expand the capabilities of spectroscopy techniques involved in remote chemical detection. The described method can be used for monitoring several fixed ground stations, which only need a mirror and lens at the location and only one spectroscopy system. Future applications include monitoring the exhaust of several chimneys of a factory, volcanic gases from vents, or monitoring product quality at various stages in a chemical or drug manufacturing factory at many fixed locations with just one remote instrument. After initial optical assembly at several fixed monitoring stations, remote analytical measurements can be performed very fast without going to any of the locations. One of the important advantages of this method is that it provides a simple approach for investigating targets on the ground which may not be visible in the direct line of sight and hence cannot be investigated using the direct laser excitation. The ATR-FR method provides a means to detect these targets using both Raman and LIBS spectroscopies.

5. References:

Acosta-Maeda, T. E., A. K. Misra, J. N. Porter, D. E. Bates, S. K. Sharma, "Remote Raman Efficiencies and Cross-Sections of Organic and Inorganic Chemicals", *Applied Spectroscopy*, DOI: https://doi.org/10.1177/0003702816668531 (2016).

Acosta-Maeda, T. E., A. K. Misra, L. G. Muzangwa, G. Berlanga, D. Muchow, J. N. Porter, S. K. Sharma, "Remote Raman Measurements of Minerals, Organics and Inorganics at 430 Meter Range", *Applied Optics*, 55 (36), 10283-10289 (2016).

Akiyama, A., Y. Morioka, and I. Nakagawa, Raman scattering and phase transition of ammonium nitrates, *Bull. Chem. Soc. Jpn.* **54**, 1662-1666 (1981).

Ali, E. M. A., H. G. M. Edwards, M. D. Hargreaves, and I. J. Scowen, Detection of explosives on human nail using confocal Raman microscopy, *J. Raman Spectrosc.*, **40**, 144-149 (2009).

Anderson, A., and Y. T. Loh, Low temperature Raman spectrum of rhombic sulfur, *Can. J. Chem.* **47**, 879-884, (1969).

Bini, R., P. Foggi, P. R. Salvi, and V. Schettino, FTIR study of vibrational relaxation in $KClO_4$ crystal, *J. Phys. Chem.* **94**, 6653-6658 (1990).

Carter, J. C., S. M. Angel, M. Lawrence-Snyder, J. Scaffidi, R. E. Whipple, and J. G. Reynolds, Stand-off detection of high explosive materials at 50 meters in ambient light conditions using a small Raman instrument, *Appl. Spectrosc*, **59**, 769-775 (2005).

Clarkson, J., and W. E. Smith, A DFT analysis of the vibrational spectra of nitrobenzene, *J. Mol. Struct.* **655**, 413-422 (2003).

Dellepiane G., and J. Overend, Vibrational spectra and assignment of acetone, ααα acetone-d_3 and acetone-d_6, *Spectrochim. Acta A* **22**, 593-614, 1968.

Ferraro, J. R., K. Nakamoto, C. W. Brown, *Introductory Raman spectroscopy*, 2nd ed; Amsterdam; Boston: Academic Press, (2003).

F. J. Fortes and J. J. Laserna. "The Development of Fieldable Laser-Induced Breakdown Spectrometer: No Limits on the Horizon". Spectrochim. Acta, Part B 2010. 65(12): 975-990.

Fraenkel, D., Structure and ionization of sulfuric acid in water, New J.Chem., 2015, 39, 5124

Furic, K., V. Mohacek, and M. Mamic, Methanol in isolated matrix, vapor and liquid phase: Raman spectroscopic study, *Spectrochim. Acta A* **49**, 2081-2087, 1993.

Gaft, M. and L. Nagli, UV gated Raman spectroscopy for standoff detection of explosives, *Optical Materials*, **30**, 1739-1746 (2008).

Gautier, G., and M. Debeau, Spectres de vibration d'un monocristal de soufre orthorhombique, *Spectrochim. Acta A* **30**, 1193-1198(1974).

Harju, M.E., Solid-state transition mechanism of ammonium nitrate phases IV, III, and II investigated by simultaneous Raman spectrometry and differential scanning calorimetry, *Appl. Spectrosc.* **47**, 1926-1930 (1993).

Harvey, P. D., and I. S. Butler, Raman spectra of orthorhombic sulfur at 40 K, *J. Raman Spectrosc.* **17**, 329-334 (1986).

Hokr B. H. , J. N. Bixler, G. D. Noojin, R. J. Thomas, B. A. Rockwell, V. V. Yakovlev, and M. O. Scully, Single-shot stand-off chemical identification of powders using random Raman lasing, PNAS, **111** (34), 12320–12324, (2014).

Laserna, J.; Lucena, P.; Ferrero, A.; Doña, A.; González, R.; Fernández, R.; de Miguel, C.; Hernández Crespo, J. (2007) Standoff LIBS Sensor Technology. Fieldable, Remotely Operated Platforms for Detection of Explosive Residues. In Prediction and Detection of Improvised Explosive Devices (IED) (pp. 18-1 – 18-18). Meeting Proceedings RTO-MP-SET-117, Paper 18. Neuilly-sur-Seine, France: RTO. Available from: http://www.rto.nato.int.

Lopez-Moreno, C., S. Palanco, J. J. Laserna, F. DeLucia Jr., A. W. Miziolek, J. Rose, R. A. Walters and A. I. Whitehouse. Test of a stand-off laser-induced breakdown spectroscopy sensor for the detection of explosive residues on solid surfaces, *J. Anal. At. Spectrom.*, **21**, 55-60 (2006).

Lutz, H.D., R. A. Becker, W. Eckers, B. G. Hölscher, and H. J. Berthold, Raman and IR spectra of the potassium, rubidium, and cesium perchlorates in the orthorhombic low-temperature modifications (baryte-type) and in the cubic high-temperature phases (sodium chloride-type with orientationally disordered perchlorate ions), *Spectrochim. Acta A* **39**, 7-14 (1983).

Mammone, J. F., S. K. Sharma, and M. Nlcol, Raman spectra of methanol and ethanol at pressures up to 100 kbar, *J. Phys. Chem.* **84**, 3130-3134, 1980.

McCreery, R.L.. ‘‘Photometric Standards for Raman Spectroscopy’’.In: J.M. Chalmers, P.R. Griffiths, eds. Handbook of Vibrational Spectroscopy. Chichester: John Wiley & Sons Ltd., 2002, pp. 1–13.

Misra, A. K., S. K. Sharma, C. H. Chio, P. G. Lucey, and B. Lienert, Pulsed remote Raman system for daytime measurements of mineral spectra, *Spectrochim. Acta A*, **61**, 2281-2287 (2005).

Misra, A. K., S. K. Sharma, P.G. Lucey, Remote Raman spectroscopic detection of minerals and organics under illuminated conditions from a distance of 10-m using a single 532 nm laser pulse, *Applied Spectroscopy*, **60**, No. 2, 223-228, (2006).

Misra, A. K., S. K. Sharma, P. G. Lucey**,** R. C. F. Lentz, and C. H. Chio, Daytime rapid detection of minerals and organics from 50 and 100 m distances using a Remote Raman system, *Proc. SPIE*, **6681**, 66810C (2007).

Misra, A. K., S. K. Sharma; D. E. Bates; T. E. Acosta, Compact standoff Raman system for detection of homemade explosives, *Proc. SPIE*, **7665**, 76650U, DOI: 10.1117/12.849850, (2010).

Misra, A. K., S. K. Sharma, T. E. Acosta, and D. E. Bates, Compact remote Raman and LIBS system for detection of minerals, water, ices and atmospheric gases for planetary exploration, *Proc. SPIE*, **8032**, 80320Q (2011); doi:10.1117/12.884392.

Misra, A. K., S. K. Sharma, T. E. Acosta, J. N. Porter and D. E. Bates, Single pulse remote Raman detection of chemicals from 120 m distance during daytime, *Appl. Spectrosc.* **66**, 1279-1285 (2012).

Misra, A. K., S. K. Sharma, T. E. Acosta, J. N. Porter, P. G. Lucey, and D. E. Bates, Portable standoff Raman system for fast detection of homemade explosives through glass, plastic and water, Proc. SPIE, 8358, 835811 (2012).

NIST, Standard Reference Database (2012) http://webbook.nist.gov/chemistry/

Oxley, J., J. Smith, J. Brady, F. Dubnikova, R. Kosloff, L. Zeiri and Y. Zeiri, Raman and infrared fingerprint spectroscopy of peroxide-based explosives, *Appl. Spectrosc*, **62**, 906-915 (2008).

Pasteris, J.D., J. J. Freeman, S. K. Goffredi, and K. R. Buck, Raman spectroscopic and laser scanning confocal microscopic analysis of sulfur in living sulfur-precipitating marine bacteria, *Chem. Geology* **180**, 3-18 (2001).

Porter, J. N., C. E. Helsley, S. K. Sharma, A. K. Misra, P. Lucey, D. Bates and B. R. Lienert, Two dimensional Standoff Raman measurements of distant samples**,** *J. Raman Spectrosc*. **43**, 165-167 (2012).

Ratcliffe, C. I. and d. E. Irish, Vibrational spectral studies of solutions at elevated temperatures and pressures.VII. Raman spectra and dissociation of nitric acid, Can. J. Chem. **63**, 3521-3525 (1985).

Sharma, S. K., P. G. Lucey, M. Ghosh, H. W. Hubble and K. A. Horton Stand-off Raman Spectroscopic Detection of Minerals on Planetary Surfaces, *Spectrochim. Acta*, A, **59**, 2391-2407 (2003a).

Sharma, S. K., J. N. Porter, A. K. Misra, H. W. Hubble, and P. Menon, Portable stand-off Raman and Mie-Rayleigh lidar for cloud, aerosols, and chemical monitoring, *Proc. SPIE*, **5154**, 1-14 (2003 b).

Sharma, S. K, S. Ismail**,** S. M. Angel**,** P. G. Lucy**,** C. P. McKay**,** A. K. Misra, P. J. Mouginis-Mark, H. Newsom, U. N. Singh, and G. J. Taylor, Remote Raman and laser-induced fluorescence (RLIF) Emission Instrument for detection of minerals, organic and biogenic materials on Mars to 100 meters radial distance, *Proc. SPIE*, **5660**, 128-138 (2004).

Sharma, S. K., A. K. Misra, and B. Sharma, Portable remote Raman system for monitoring hydrocarbon, gas hydrates and explosives in the environment, *Spectrochim Acta* A, **61**, 2404-2412 (2005).

Sharma, S. K., P. G. Lucey and A. K. Misra, Stand-off Detection of Explosives with Remote Raman Spectroscopic Technique, *Proceedings of the 7th Intl. Symposium Mine Symposium on Technology and Mine Problems,* Naval Postgraduate School, Monterey, CA, May 2-5, pp10 (2006 a). (FOUO)

Sharma, S. K., A. K. Misra, P. G. Lucey, S. M. Angel, C. P. McKay, Remote pulsed Raman spectroscopy of inorganic and organic materials to a radial distance of 100 meters, *Appl. Spectrosc.* **60**, 871-876 (2006 b).

Sharma, S. K., J. N. Porter, A. K. Misra, C. E. Helsley and D. E. Bates, Scanning time-resolved stand-off Raman instrument for large area mineral detection on planetary surfaces, European J. Mineral. **25**, 715-720 (2014).

Stephenson, C.V., W. C. Coburn, Jr., and W. S. Wilcox, The vibrational spectra and assignments of nitrobenzene, phenyl isocyanate, phenyl isothiocyanate, thionylaniline and anisole, *Spectrochim. Acta* **17**, 933-946 (1961).

Stokes, R. J., W. E. Smith, B. Foulger and C. Lewis, Rapid screening and identification of improvised explosive and hazardous precursor materials by Raman spectroscopy, *Proc. SPIE*, **7119**, 71190/1 - 71190/9 (2008).

Troupry, N., H. Poulet, M. Le Postollec, R. M. Pick, and M. Yvinec, A Raman spectroscopic study of the structural phase transition and reorientational motions of the ClO_4^- ions in $KClO_4$, *J. Raman Spectrosc.* **14**, 166-177 (1983).

Wright, C. W., S. D. Harvey, and B. W. Wright, Detection of hazardous chemicals using field-portable Raman spectroscopy, *Proc. SPIE*, **5048**, 107-118 (2003).

6. Distribution Statement:

- DISTRIBUTION A. Approved for public release: distribution unlimited.

7. Publications:

1. Misra A.K., T. E. Acosta-Maeda, J. Porter, G. Berlanga, D. Muchow, S. K. Sharma, B. Chee. Two Components Approach for Long Range Remote Raman and LIBS Spectroscopy Using Low Laser Pulse Energy, Applied Spectroscopy, in print 2018.
https://doi.org/10.1177/0003702818812144

8. Technology transfer

Patent disclosure filed:

REPORT OF INVENTIONS AND SUBCONTRACTS

Name of Contractor: University of Hawai'i
Contract: N00014-15-1-2575

SECTION I – SUBJECT INVENTIONS

5a. NAME(S) OF INVENTOR(S)	5b. TITLE OF INVENTION(S)	5c. DISCLOSURE NUMBER, PATENT APPLICATION SERIAL NUMBER	5d. ELECTION TO FILE PATENT APPLICATIONS 1. UNITED STATES	5d. ELECTION TO FILE PATENT APPLICATIONS 2. FOREIGN	5e. CONFIRMATORY INSTRUMENT OR ASSIGNMENT FORWARDED TO CONTRACTING OFFICER
Misra, Anupam Sharma, Shiv K. Porter, John Acosta-Maeda, Tayro Helsley, Charles E.	Novel method for fast, long range remote chemical detection using low cost toy cars, drones and simple ground stations	UH 01070	N	N	N
Misra, Anupam Porter, John Acosta-Maeda, Tayro	Long range remote chemical detection using compact spectroscopy system	UH 18/0024, 62/618,280	N	N	N

9. Participants:

1. Dr. Anupam Misra (Faculty)
2. Dr. Tayro Acosta-Maeda (Postdoctoral fellow, later became faculty)
3. Dr. John Porter (Faculty)
4. Dr. Shiv Sharma (Faculty)
5. Mr. Brian Chee (IT specialist)
6. Mr. Mark Wood (Electronics and software engineer)
7. Mr. Genesis Berlanga (Graduate Student)
8. Mr. Dalton Muchow (Undergraduate student)